12-2016

Windshield Defrost and Deice Using Carbon Nanotube Composite

Santhosh Kumar Loganathan

WINDSHIELD DEFROST AND DEICE USING CARBON NANOTUBE COMPOSITE

A Thesis

Submitted to the Faculty

of

Embry-Riddle Aeronautical University

by

Santhosh Kumar Loganathan

In Partial Fulfillment of the

Requirements for the Degree

of

Master of Science in Aerospace Engineering

December 2016

Embry-Riddle Aeronautical University

Daytona Beach, Florida

WINDSHIELD DEFROST AND DEICE USING CARBON NANOTUBE

COMPOSITE

by

Santhosh Kumar Loganathan

This thesis was prepared under the direction of the candidate's committee chairman, Dr. Virginie Rollin and co-chairman Dr. Daewon Kim, Department of Aerospace Engineering, and has been approved by the member of the thesis committee Dr. Jeff Brown, Department of Civil Engineering, Daytona Beach Campus. It was submitted to the School of Graduate Studies and Research and was accepted in partial fulfillment of the requirements for the degree of Master of Science in Aerospace Engineering.

THESIS COMMITTEE

Chairman, Dr. Virginie Rollin

Co-chairman, Dr. Daewon Kim

Member, Dr. Jeff Brown

Department Chair, Dr. Anastasios Lyrintzis
or Graduate Program Coordinator, Dr. Magdy Attia

11.16.2016
Date

Dean of College of Engineering, Dr. Maj Mirmirani

11/16/2016
Date

Vice Chancellor, Academic Support, Dr. Christopher Grant

11/16/16
Date

ACKNOWLEDGMENTS

It gives me pleasure to acknowledge the people that made this research successful. I would like to express my deepest gratitude to Embry-Riddle Aeronautical University and my thesis advisors, Dr. Virginie Rollin and Dr. DaeWon Kim for providing the resources and endless support in sharing their expertise to conduct this research.

In addition, I specially acknowledge Dr. Jeff Brown for serving on the committee and his support in the thermography facility. I also acknowledge Mr. Mike Potash for his helpful discussions on electrical components and electrical principles involved in this thesis. His advice and suggestions have been invaluable.

I would also like to thank my NRG group mates who have helped me in the process of this thesis. I also appreciate the financial support of Embry-Riddle Aeronautical University to conduct this experiment through an internal grant (Grant No. 13255) and provided the equipment facility to conduct this research in an efficient way. I also want to acknowledge the support of the National Science Foundation through the use of the Scanning Electron Microscope purchased with award # 1337742.

I would like to express my sincere gratitude to Dr. Stephanie Miller and patent attorneys for preparing the patent report and filing it.

Finally, I would like to thank my brother Arul Kumar Loganathan and my parents for their financial and immense moral support to pursue my Master of Science in Aerospace Engineering.

TABLE OF CONTENTS

LIST OF TABLES

LIST OF FIGURES

SYMBOLS

$°C$	Degree Celsius
S/m	Siemens per meter
μm	Micrometer
nm	Nano meter
mm	Millimeter
T	Temperature
T	Transmittance
P_d	Surface power density
I	Current
V	Voltage
A	Area
Ω	Ohms
ΔT	Temperature difference

ABBREVIATIONS

CNT	Carbon Nanotube
SWNT	Single-Walled Nanotube
DWNT	Double-Walled Nanotube
MWNT	Multi-Walled Nanotube
TCF	Transparent Conductive Film
ITO	Indium Tin Oxide
NTC	Negative Thermal Coefficient
UV	Ultra-Violet
EDX	Energy-Dispersive X-ray Spectroscopy
CVD	Chemical Vapor Deposition
RF	Radio Frequency
DC	Direct Current
SEM	Scanning Electron Microscope
RGB	Red Green Blue

ABSTRACT

Carbon nanotubes (CNT) are well known for their high thermal and electrical conductivities and can offer a great advantage by converting the applied electrical energy into instant heat with minimum energy loss. The goal of this research is to develop a very thin CNT layer sandwiched between two layers of glass substrate in order to generate instant heat through electrodes. The thin CNT layer is fabricated using the CNTRENE^{TM} solution, which is a mixture of single-walled nanotubes (SWNTs) (~75%), double-walled nanotubes (DWNTs), and multi-walled nanotubes (MWNTs) with an average CNT length of ~0.4 - 0.6 μm. The thin layer is deposited by spin coating the CNTRENE^{TM} solution on the transparent glass substrate. By varying the number of coated layers, the effects of optical transmittance and heating rates are observed. Results show that a room temperature specimen reaches 60 °C within 80 seconds, reproducing the same results over time. This technique can be used to develop a transparent conductive film heater, particularly for defrosting or deicing windshields, and can also be applied to other surface types that need instant heating. This research can replace conventional heaters, Indium Tin Oxide (ITO), which are fabricated either by dielectrophoresis or piece-wise alignment.

1. Introduction

This research was in the field of a unique material called carbon nanotubes, known for their thermal, electrical, and mechanical properties. In this research, a scaled prototype model of windshield defrost and deice system was designed, manufactured, and tested. In the past few decades, the application of carbon nanotubes has been studied in various fields. This thesis will explain a recent development of carbon nanotubes for defrosting, demisting, and their applications.

1.1. Prior Research

The need for a transparent conductive film (TCF) and transparent heating glass has increased in a wide range of applications, such as solar voltaic cells, thermally-based sensors and window defroster and deicers. The current market demand for transparent heaters has vastly increased. This type of transparent heaters was made up of an optically transparent conductive film that was achieved by any type of coating mechanism.

1.1.1. Indium Tin Oxide Heater

Indium tin oxide (ITO) is one of the transparent heaters which fulfills the current market demand for transparent heaters (Transmittance, T >95%). An aircraft defrosting and demisting system using an ITO coating has been patented by Briggs (Briggs, 2004). In this system, a resistive coating of ITO was positioned between transparent sheets. The transparent sheets could be comprised of polycarbonate, polyvinyl butyral or glass. The AC current was applied to the thin resistive ITO coating to generate heat, which results in avoiding the accumulation of mist and ice on the windshield. This resistive coating has a resistivity of 50 Ω/m^2, 25 Ω/ m^2, or 10 Ω/ m^2, based upon the requirements.

Many scholarly journals have been published about ITO heaters in windscreens. However, these ITO heaters also have disadvantages, such as slow thermal response, being very brittle, and having a high manufacturing cost, which was described by previous authors (Coutal and Azema, 1996). Various research activities have been carried out to overcome these disadvantages (Wu and Chen, 2004). There are still many problems to overcome before commercializing them; one of them being the interference of the ITO coating with radio transmissions, as this adversely affects radio and mobile phone reception (Rajamani, Stelson and Cui, 2006). Moreover, engineers have pointed out that cloudiness, humidity, wind, and regular washing fluid could affect the performance of the coating, in addition to the high expense of the ITO (Park and Kim, 2015).

1.1.2. Carbon Nanotubes Heater

More recent studies have revealed the development of optically transparent heaters using carbon nanotubes due to their excellent optical transparency (applied as a very thin layer), high electrical conductivity (10^6 S/m), mechanical flexibility, and the abundance of availability (Jang, Jeon and Nahm, 2011).

One recent publication (Wu, Chen, Logan and Tanner, 2004) described a simple fabrication method of ultrathin films using optically homogeneous and electrically conductive single walled carbon nanotubes. This process utilized a unique mass fabrication method to increase the availability of carbon nanotubes at the commercial scale. The manufactured sheet showed a higher optical transmittance than the sheet made up of indium tin oxide, with a similar electrical resistance. The manufactured film indicated the broad capability of applications such as photonic devices and optical modular sensors. Due to the degrading life time performance this method is not commercialized.

Carbon nanotubes are composed of carbon atoms and hence they can be oxidized at very high temperature. However, carbon nanotubes are thermally stable in an oxygen environment up to 350°C. Beyond this temperature, they may degrade due to oxidation of the carbon atoms. In a vacuum, carbon nanotubes endure temperatures up to 3726°C due to the extreme strength of the sp2 hybridized carbon-carbon bond. This property makes it more suitable for developing transparent heaters (Kang, Seo and Park, 2010). It has been proven that carbon nanotubes exhibit advantages over indium tin oxide, such as ease of mass production, low product cost per unit, enhanced thermal and chemical stability. These parameters help to overcome the issue faced by indium tin oxide based transparent heaters and provide an opportunity to use them in wide range.

Some researchers (Rajamani, Stelson and Cui, 2006) worked on developing a carbon nanotube based transparent thin film acoustic actuators (speaker) and sensors (microphone). In their experiments, a transducer consisting of a piezoelectric poly-vinylidene fluoride thin film is used to develop the substrate. It was coated with carbon nanotube based transparent conductors, which are fabricated by carbon nanotube acid treatment. The fabricated thin film transducers showed an excellent radio frequency transparency over a broadband frequency range, and have the advantages of being transparent, flexible, extremely thin, and lightweight. A 250 mm × 190 mm transparent thin film actuator/sensor used in their research is shown in Figure 1.1.

Figure 1.1 A 250 mm × l90 mm transparent carbon nanotube thin film actuator/sensor (Rajamani, Stelson and Cui, 2006)

A recent patent (Wang and Liu, 2013) showed that it was possible to use carbon nanotubes as a windshield heater for demisting and defrosting. The defrosting window includes transparent glass, an adhesive layer on which a carbon nanotube film is attached, two electrodes and a protective layer. The top surface was a transparent substrate and a protective layer was used to isolate the carbon nanotube heater from atmospheric contact. This protective layer protects both the carbon nanotubes and electrodes, but the heat loss was high due to high glass thickness. Due to the slow fabrication process and insufficient results, their product was not commercialized. The schematic setup of this windshield is shown in Figure 1.2. Also, the CNTs cover a very small area.

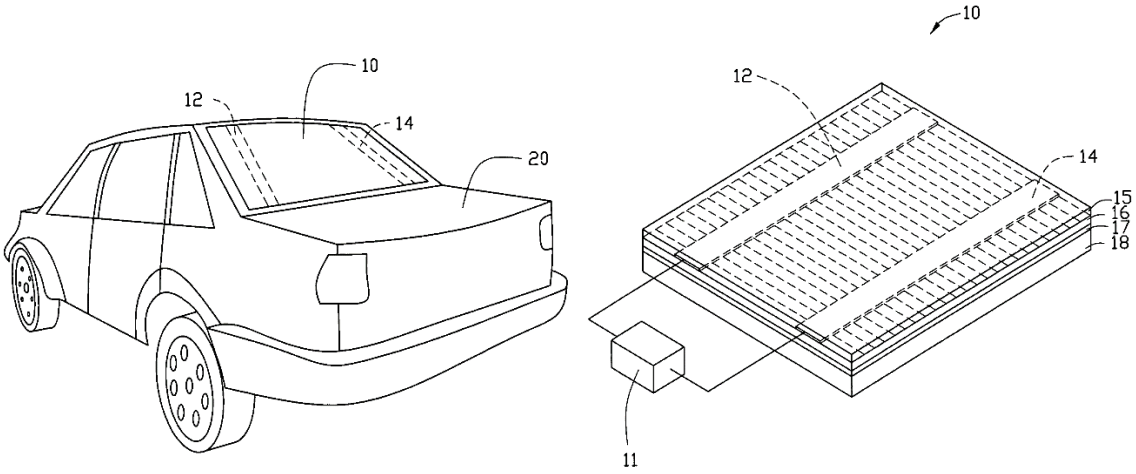

Figure 1.2 Schematic diagram of the rear windshield defrost system (Wang and Liu, 2013)

In another study, a simple transfer method of carbon nanotubes was demonstrated (Jung, 2013), to cover the entire surface area. In this experiment, single-walled carbon nanotubes are used as a heater because of their better thermal conductivity than multi-walled carbon nanotubes but this resulted in some issues in purification, separation, and dispersion in liquid. The multi-walled carbon nanotubes sheet heater was fabricated using a super-aligned multi-walled carbon nanotubes forest and directly coated onto a glass substrate. One layer, three layer, and five layer multi-walled carbon nanotube sheets were manufactured with sheet resistance of 756 Ω/m^2, 342 Ω/ m^2 and 172 Ω/ m^2, respectively. The manufactured heater is shown in Figure 1.3.

Figure 1.3 Ribbons of carbon nanotube are pulled out from silicon substrate and transferred to the heater (Jung, 2013)

To overcome the expensive nature of carbon nanotubes, it should be mass manufactured. A publication presented by (Kumar and Ando, 2010) shows the method to mass produce the carbon nanotubes. In this research, a method for mass producing multi-walled carbon nanotubes using chemical vapor deposition was explained in detail. Parameters to grow carbon nanotubes such as carbon precursor, metal catalyst, particle size, temperature, and pressure are given. A small change in these parameters can severely alter the carbon nanotube manufacturing process. It was suggested that due to the demand of carbon nanotubes in the near future, it was necessary to look for a method to manufacture carbon nanotubes using renewable sources of energy. The manufactured multi-walled carbon nanotube forest is shown in Figure 1.4.

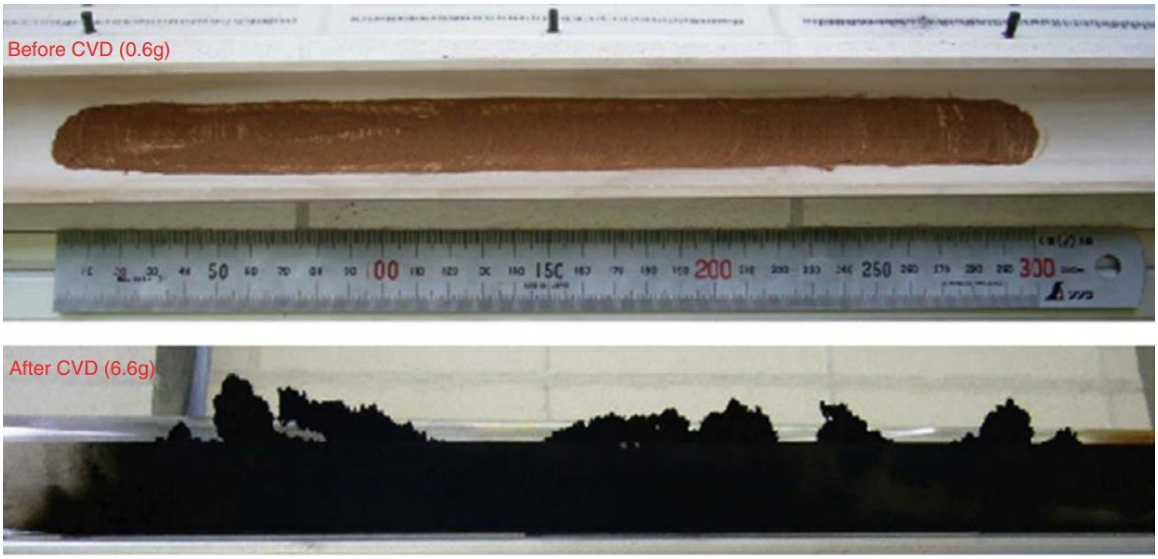

Figure 1.4 Photographs of the carbon nanotube bed before and after chemical vapor deposition (Kumar and Ando, 2010)

In another publication, (Wu and Wang, 2009), proposed a method to prepare a large area of double walled carbon nanotube film and to apply it as a film heater. In this study, a large area of carbon nanotube film was manufactured and high heating efficiency values were observed. It was also noticed that using double walled carbon nanotubes can save 20 - 30% of energy and using single walled carbon nanotubes can save 25 – 35% (Kang, Kim, and Seo, 2011) of energy when compared to conventional metal heaters for the same power input. This is due to the fact that single walled nanotubes have less surface area and can make more interaction or contact points than the double walled nanotubes. Also, the film was manufactured in different shapes and thicknesses. It was also proposed that high heating performance was possible by using a large entangled network of carbon nanotubes. The major problem in this process was the manufactured film was not transparent enough. The manufactured DWCNT film is shown in Figure 1.5.

Figure 1.5 Optical image of a large-area DWCNT film about 30 × 30 cm^2 (Wu and Wang, 2009).

A recent study (Janas and Koziol, 2014) showed a method to manufacture ultra-fast carbon nanotube heaters with improved performance. The film was synthesized on the roller and cut in the form of sheets. The ultra-fast carbon nanotube film that was used to convert electric power into heat with very high efficiency was manufactured from aerogel. Acetone was used to enhance the electro thermal properties of the carbon nanotubes. A single droplet of acetone was dropped on the film to increase the thermal efficiency. The manufactured CNT sheet from the roller method is shown in Figure 1.6.

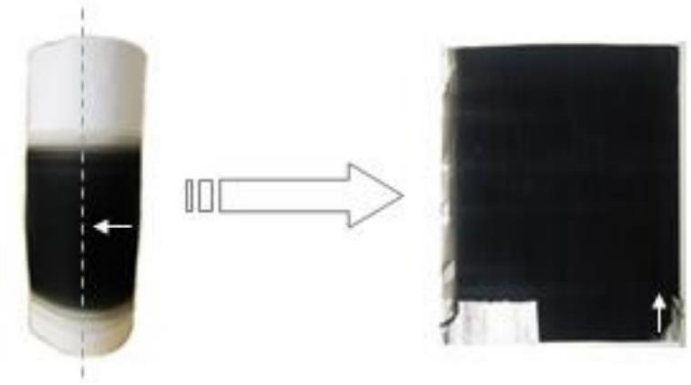

Figure 1.6 CNTs collected on the roller and cut into sheet (Janas and Koziol, 2014)

1.2. Joule Heating Effect

If we apply electric current through any conductive material, then the applied electric current will induce Joule heating effect or self-heating or resistive heating. The phenomenon is that the electric current will cause the traveling electrons to bounce off the atoms of the conductive element and make them vibrate. This vibration rate will create the rise in temperature. A tungsten filament inside an incandescent light bulb is one of the best examples that uses this principle to produce light. The thermal output will vary depending upon the conductive nature of the element. A highly conductive material will produce less Joule heating effect whereas a highly resistive material will produce a high Joule heating effect.

Recently, Joule heating effect was experienced by (Chen, Cho and Kumar, 2014) while testing the electrical conductivity of polyacrylonitrile carbon nanotube composite fibers. In this research, the polyacrylonitrile carbon nanotube composite fibers with 15% and 20% carbon nanotubes were manufactured. These fibers' electrical properties were enhanced by an annealing process at different temperatures. With the application of various electric current ratings at fixed length, the carbon nanotubes exhibit the Joule heating effect. A Schematic diagram of Joule heating around carbon nanotube is shown in Figure 1.4.

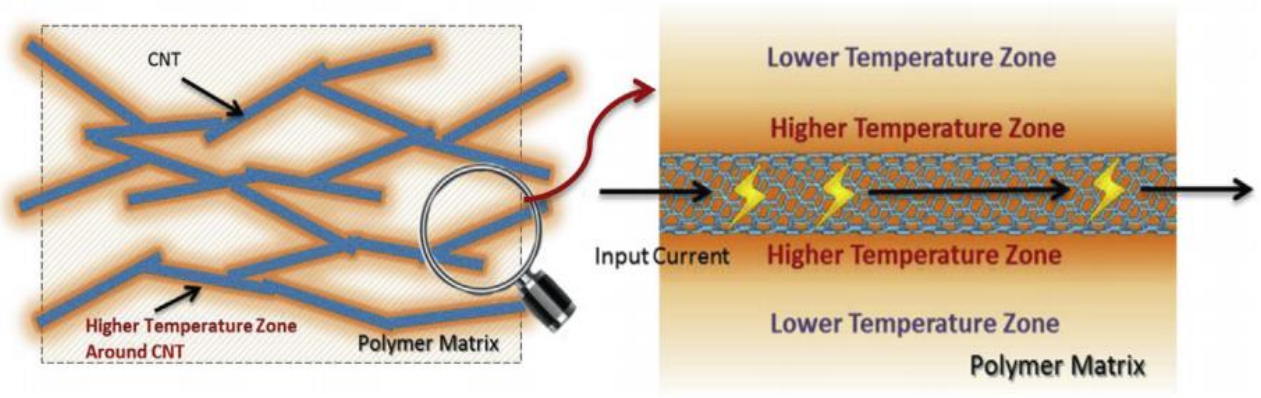

Figure 1.7 Schematic diagram of Joule heating around carbon nanotube (Chen, Cho and Kumar, 2014)

Carbon nanotubes are excellent electrical conductors by nature, they tend to produce low resistive heating effect. The performance can be increased by functionalizing the carbon nanotubes (see Chapter 3). There are many elements available to functionalize carbon nanotubes. One of the ways to increase the Joule effect is to functionalize the carbon nanotube with a good insulator.

1.3. Need for New Approach

One of the drawbacks of previous CNT-based transparent heaters was scaling up the manufacturing process, which was encountered by previous researchers (Jung, Kim and Lee, 2013). The method claims that the CNTs were grown on the sheet in the chemical vapor deposition (CVD) apparatus. In transparent heaters, it should be done directly on the glass substrate, but the problem is that it is not possible to grow CNTs on an entire windshield, as there was no CVD apparatus large enough. A possible solution could be growing the CNTs on silica wafers and transferring them to the actual windshield, which can cause non-uniformity and layer deterioration. The described method is neither time nor cost effective (Jung, Kim and Lee, 2013).

2. Objectives and approach

The objective of this research was to design a scaled model of a windshield defrost and deice system that is more amenable to large-scale manufacturing. Also, it would provide a swift operation to overcome the accumulation of mist or ice on the windshield surface. Conventional systems include different trustworthy and expensive equipment such as indium tin oxide film.

The improved reliability and immediate response time of the model were also important parameters that were investigated during this research. Also, the lifetime performance was analyzed. If the CNT coating performance degrades through its lifetime, it will have a reduction in its overall operation efficiency. The research flowchart with different stages is shown in Figure 2.1.

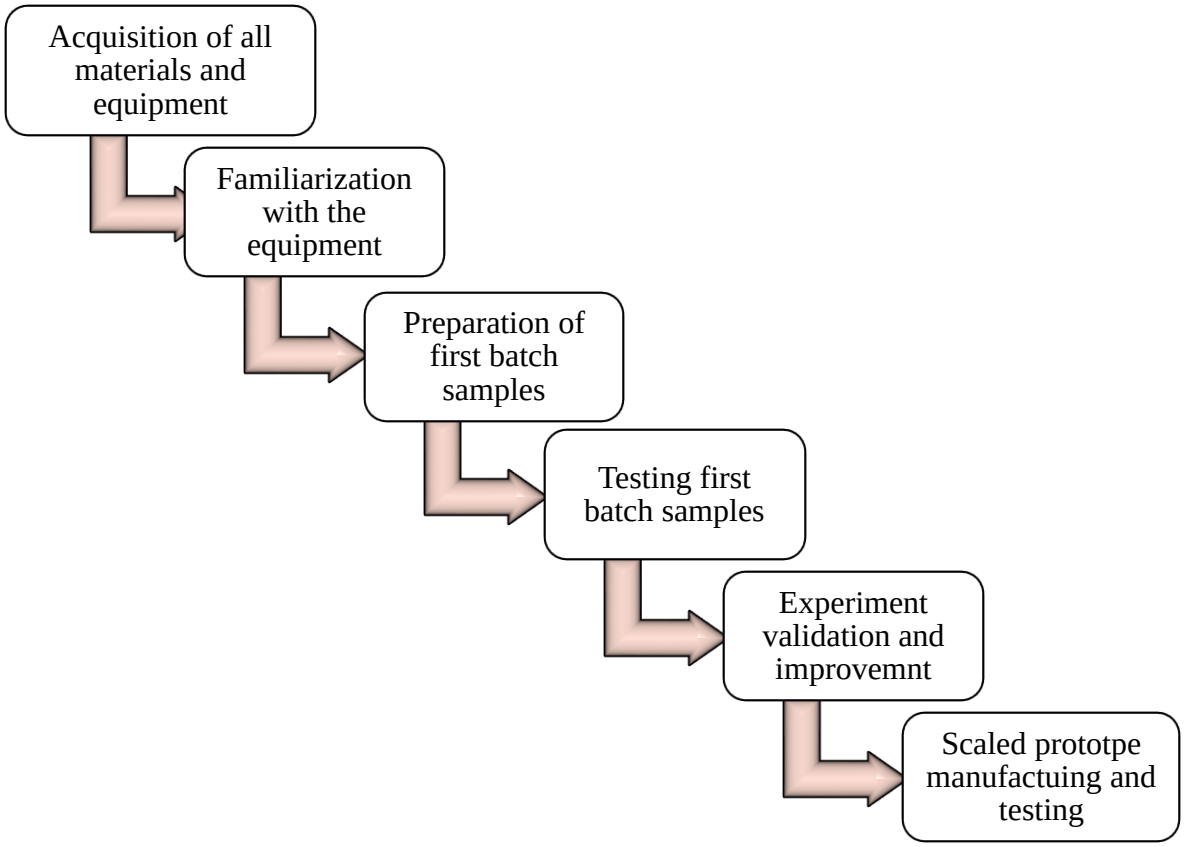

Figure 2.1 Flow chart with forecasted research stages

The objectives of this research are carefully listed and the different stages of experiments and developments are forecasted in the initial stage. The application of the CNTRENE™ (see Chapter 3) solution was first experimented in the lab. Then the principle of applying the current to the CNT layer for this application was experimentally verified. Later, the scaled model was developed with input from the preliminary experimental results.

2.1. Schematic Setup

The typical setup would consist of four layers of engineering materials. The first layer was the actual windscreen glass. The second layer was the carbon nanotube layer measuring a few micrometers of thickness. The third layer was the electrodes, which were attached on the edges. The electrodes are made up of copper or silver depending upon the final product requirement. The fourth layer was another windscreen glass. The fourth layer could be replaced with a specially designed, non-reactive protective coating or an anti-scratch, high thermal performance one-sided tape, as will be discussed later. Figure 2.2 shows the schematic setup of transparent glass heater where the CNT film and copper electrodes are sandwiched between two glass substrates.

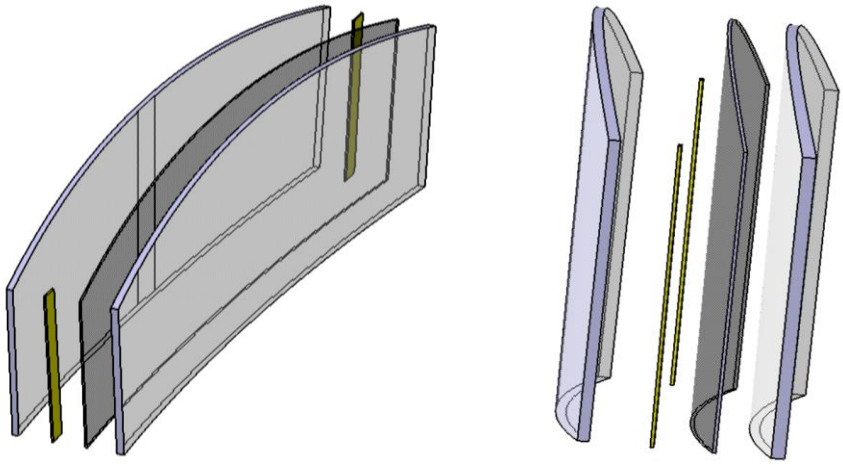

Figure 2.2 Schematic diagram of CNTRENE™ sandwiched transparent glass is designed using CATIA

2.2. Coating Methods

There are different methods by which the CNTRENE^{TM} coating can be applied on the surface of the glass to develop the transparent heater. The preferred method can vary based on the desired coating scale area and precision. It was important to study those coating methods to produce the desired results.

2.2.1. Dip Coating

The process of a continuous bath immersion was used where the substrate is dipped in the coating material. The dip coating method allows easy control of thickness. This is done by adjusting different variables including number of dips, withdrawal velocity, substrate surface characteristics, contact angle of the solution to the substrate, solution temperature, and the concentration rate of the solution to be coated. This method is very suitable for large-scale double-sided coating with high uniformity and precision thickness control but this process is time consuming. The dip withdrawal should be done at a constant rate in order to avoid micro pattern marks. Because the coating needs to be on one side of the glass substrate only, this process is not recommended for this research and was not investigated further.

A recent publication (Chen, Zhong, and Wang, 2016) stated that using the dip coating method could produce a large area of OLED light panel with panel size of 86 × 86 mm^2. Films with a thickness of 40 nm were having a non-uniformity of 17-18%, which was less than that of other methods. Due to a very uniform coating, the light emission uniformity and performance was remarkable. Figure 2.3 shows the graphical abstract of the dip coating process by (Chen and Wang, 2016).

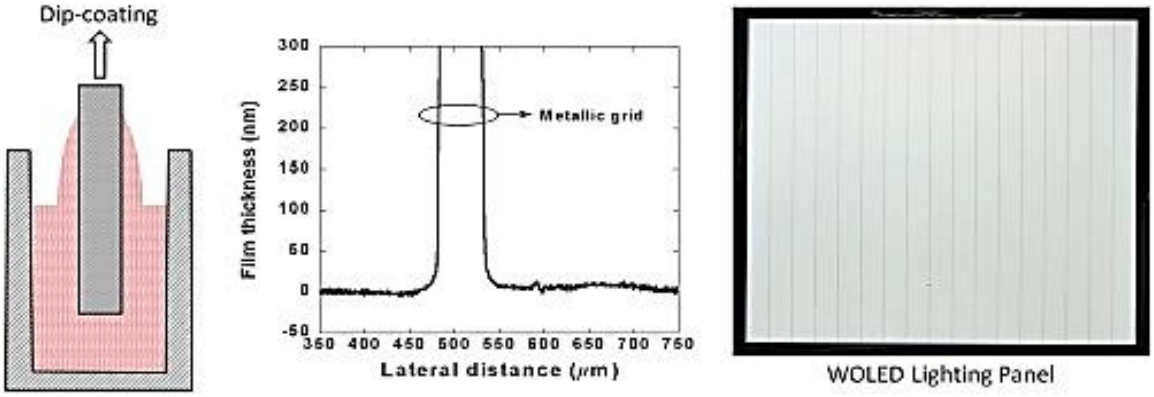

Figure 2.3 Graphical abstract of the dip coating concept (Chen and Wang, 2016)

2.2.2. Spray Coating

Spray Coating has been well-established for more than a decade in industrial coating. This large area coating technique ensures the ideal coating for solution deposition with different surface morphologies, which was more often used for inline manufacturing. Moreover, the wastage of the solution was reduced to minimal quantities and, by shadow masking techniques, it could be possible to produce a desired pattern. Also, by using the spray coating technique, it was possible to access the broad spectrum of solutions with different rheological properties.

A recent publication (Won and Son, 2016) explained the advantage of spray pyrolysis technique to coat with nano particles. In spray pyrolysis technique, an ultrasonic transducer at the tip of the nozzle atomizes the solution, which is then deposited on the substrate surface, as shown in Figure 2.4.

Parameters, like lateral velocity, dispensing rate, speed of the spray head movement, and the number of consecutive sprays, would determine the thickness of the layer. A superior amount of control over the processing with additional equipment, such as an automated and computer controlled spray coater, should allow for an improved performance.

Figure 2.4 Spray pyrolysis equipment with ultrasonic transducer is used for spray coating procedure (Holmarc Pvt. Ltd.)

2.2.3. Spin Coating

The simple spin coating process has been used for decades as a method to produce or apply very thin films on the substrate surface. The most common methods of spin coating are the static dispense method and the dynamic dispense method. Generally, a small puddle of fluid is dropped at the center of the spinning substrate. Most of the liquid dispensed on the surface goes off of the substrate edge. This is due to the centripetal force created by the rotating disc.

The thickness of the final film depends on multiple parameters, which include the spin time, spin RPM, acceleration rate, surface tension of the solution, amount of solution, evaporation rate, and the atmospheric temperature. In order to achieve the desired thickness and precision, it is important to perform the spin coating in a controlled environment. One of the main advantages of spin coating is the repeatability and scalability. One downside is that a large amount of solution is wasted as it spreads over the side of the sample.

In the static dispense method, a small puddle of solution is dropped at the center of the substrate while the stage is in static condition. The amount of solution depends upon the concentration and area of the substrate. In the dynamic dispense method, a small puddle is applied on the substrate, mostly in the center while the stage is rotating. Due to the nature of this research, spin coating was apt to meet the goal requirements. Henceforth, this research proceeds with a modified static dispense spin coating technique.

A typical spin coating process contains four steps, which are described in Figure 2.5. In the first step, the substrate is loaded on the stage. In the second step, the coating solution is dispensed on the substrate surface. In the third step, film casting and settling process is achieved, where the applied solution disperses and covers the entire surface. The final step is the completion stage where spinning occurs. Depending upon the level of complexity in this process, additional steps may involve film curing and isolation. In this research, we modify slightly the static dispense technique, as will be explained in Chapter 4.

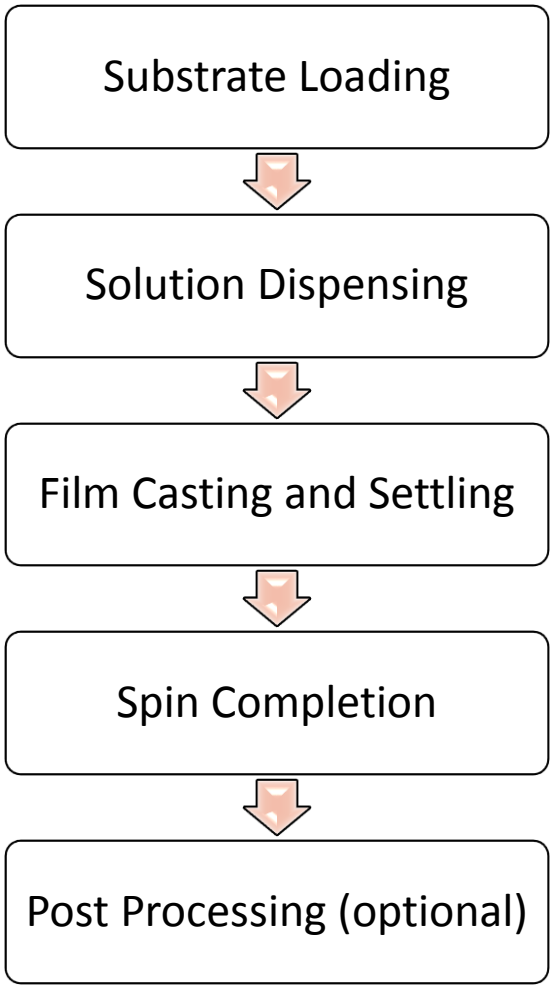

Figure 2.5 Flowchart explains the simple spin coating step by step process

3. CNTRENE™ Solution

In order to achieve maximum heating efficiency, the conductive layer was modified in such a way as to achieve high temperature with minimum voltage. This could be achieved by functionalizing the CNTs with sulfur since it is an excellent electrical insulator. CNTRENE™ 3021 B3-R is a product engineered by Brewer Science for this specific purpose. To functionalize the CNTs with sulfur, it is necessary to introduce carbon and sulfur-based gases during the growth process. Sulfur is insoluble in water and most solutions except for carbon disulfide. Therefore, functionalization was performed, most likely by introducing the carbon disulfide gas, which was the source of sulfur, along with the gasses to manufacture carbon nanotubes. This was done by Brewer Science and they remained quite secretive about CNTRENE™, so we spent some time learning more about the solution.

3.1. Introduction to solution

The solution contains a mixture of sulfur-functionalized single-walled nanotubes (SWNT, ~75%), double-walled nanotubes (DWNT) and multi-walled nanotubes (MWNT) with ammonium hydroxide and water. It is important to examine the solution before performing the spin coating method. The examination was done by using the energy-dispersive X-ray spectroscopy (EDX) attachment in the scanning electron microscope. For this research, we used the Bruker EDX scan system in our FEI Quanta 650 scanning electron microscope. The research will show how the EDX system was used to determine the qualitative composition of the CNTRENE™ solution.

3.2. Energy-Dispersive X-ray Spectroscopy Scan (EDS or EDX)

The surface morphology of any material and its chemical composition can be studied by using EDX. This method is based on the X-ray source interaction upon the sample material surface. A high beam of electron source is focused on the sample and will excite an atom from an unexcited ground state. Then, the electrons from the outer high-energy shell will fill the gap. This tends to create an energy difference and releases an X-ray. This energy difference is measured by the analyzer in the EDX system. Each element in the periodic table holds its own energy spectrum, which is measured and displayed on the monitor.

3.3. Composition

Elemental analysis of the CNTRENE^{TM} solution was performed using an EDX scan, where EDX is used to measure qualitative and quantitative elemental composition at the nanoscale. 0.5 ml of the CNTRENE^{TM} solution was dropped on an aluminum stub and left to dry for 24 hours, as shown in Figure 3.1. The prepared specimen was then loaded into the SEM to perform the EDX test.

From the experiment, we confirmed that sulfur was present in the solution, confirming the doping process of the CNTs. Figure 3.2 shows the EDX spectrum is portrayed as a plot of X-ray counts vs. energy (in KeV). The test also reveals the presence of aluminum and oxygen. It was concluded that the presence of oxygen was due to the ammonium hydroxide. The presence of sulfur was due to the functionalization of the carbon nanotubes. The high concentration of aluminum was coming from the stub.

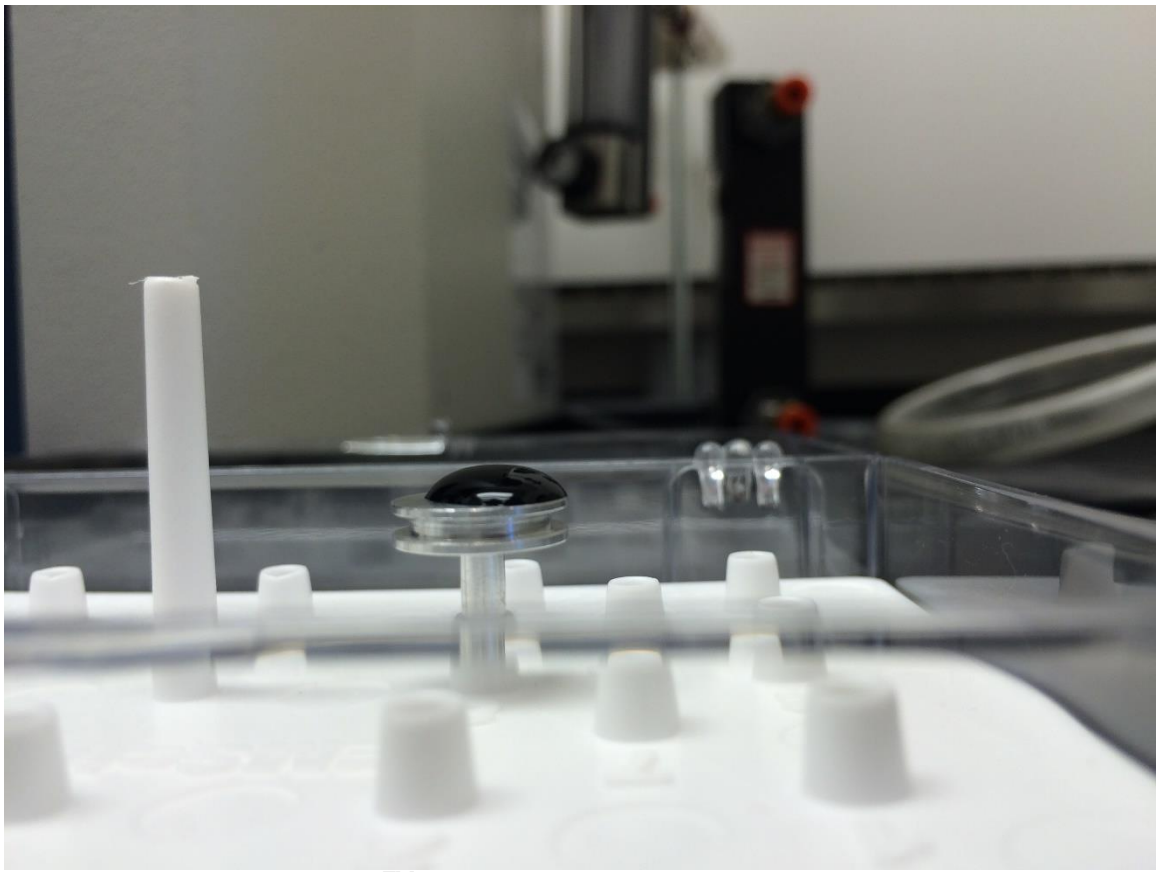

Figure 3.1 CNTRENE^{TM} sample in aluminum stub for performing EDX

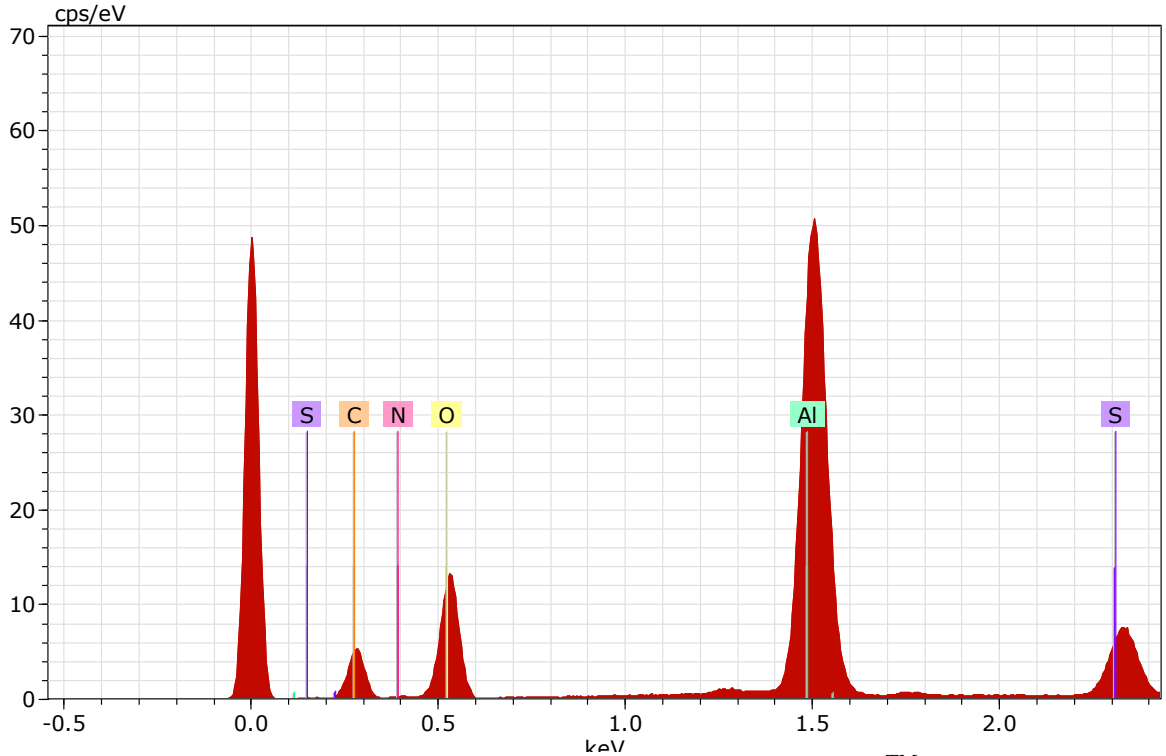

Figure 3.2 EDX is performed on the specimen with CNTRENE^{TM} solution

3.3.1. Sulfur

The above data from the EDX scan exhibits the presence of sulfur in the solution. By nature, sulfur is a good insulator and the electrical resistivity of sulfur is very high (1×10^{15} Ω m). Also, the boiling point is 444 °C, hence it is very stable for our research requirements. A new EDX scan was performed on the glass surface after spin coating the CNTRENE^{TM} solution. In order to see the CNTs, the scan runs on one of the glass edges. Therefore, it was difficult to see the CNTs on the perfect surface. Figure 3.3 shows the EDX scan area. Figures 3.4 and 3.5 show the presence of carbon and sulfur, respectively. It was observed that, under perfect coating conditions, the CNTs are evenly distributed on the surface, as is sulfur. This makes sense if the CNTs are functionalized with sulfur, meaning sulfur atoms are attached to the CNTs.

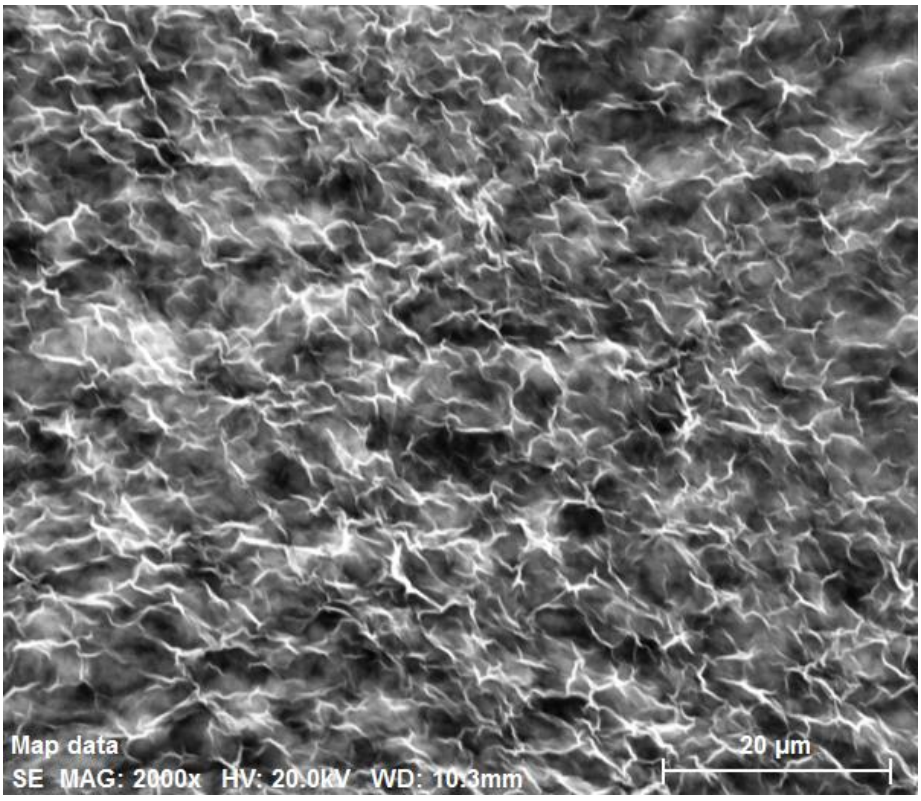

Figure 3.3 EDX scan area on the spin coated glass surface

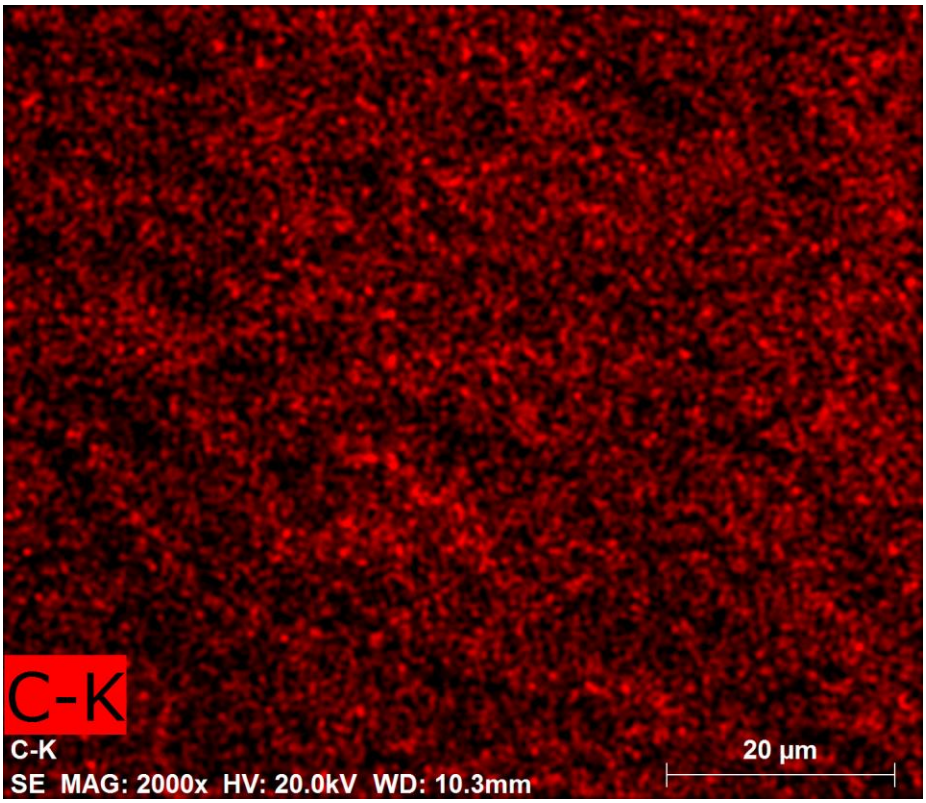

Figure 3.4 The concentration of carbon element on the scanned area

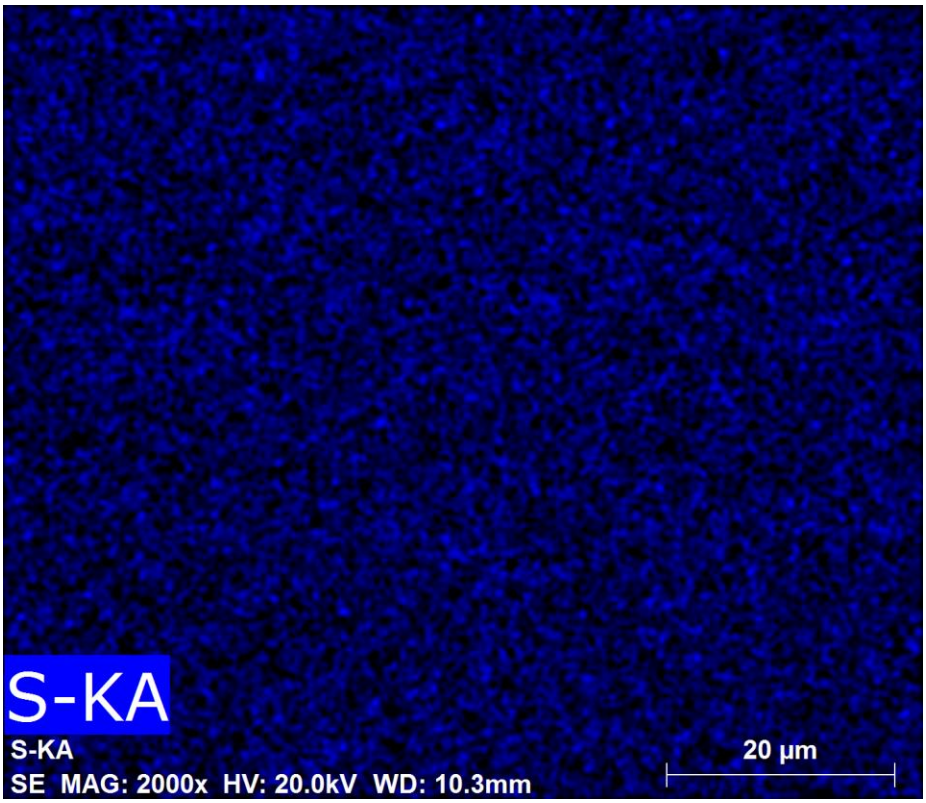

Figure 3.5 The concentration of sulfur element on the scanned area

The layer of carbon nanotubes creates a very effective connection between the two electrodes. The presence of sulfur in the solution makes the coating an excellent resistor. This helps produce a high temperature output for the applied voltage, compared to previous studies (Kim and Seo, 2011).

3.3.2. Ammonium Hydroxide

The presence of nitrogen and oxygen in the EDX scan chart was due to ammonium hydroxide [NH_4OH] in the solution. Hydrogen cannot be detected using an EDX scan, and is thus absent from the results. There are multiple reasons for the use of ammonium hydroxide (Thomas R, 1991). The first and foremost is a dispersive effect. The functionalized carbon nanotubes are more prone to attract and stick together with nearby carbon nanotubes, but this can be prevented by using an ammonium hydroxide solution.

The second important function of the use of ammonium hydroxide is that it will create a hydroxide environment by engaging all hydrogen and oxygen elements in the solution. The name ammonium hydroxide shows an alkali with composition: [NH_4^+] [OH^-]. This, in turn avoids the formation of sulfur dioxide and carbon dioxide gases, from the reaction shown below. Sulfur dioxide is highly toxic gas with a pungent and irritating smell.

$$CS_2 + 3O_2 \rightarrow CO_2 + 2SO_2$$

The third reason is to provide a uniform coating during the spin coating process. The surface tension of ammonium hydroxide is very low and this makes the solution spread more freely on the glass surface. Also, it could provide an additional bonding effect between the self-adhering carbon nanotubes and the substrate surface. Figure 3.6 shows the presence of nitrogen on the CNTRENE^{TM} coated glass surface. Also, the amount of

elements in the entire scan area is shown in table 3.1.

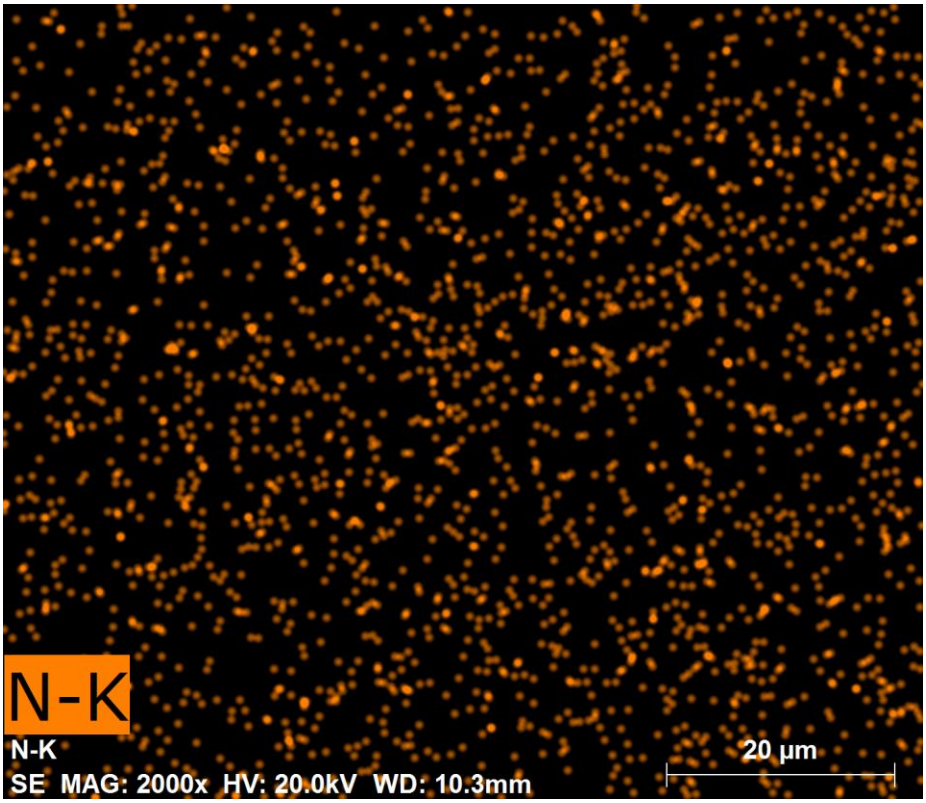

Figure 3.6 The concentration of nitrogen element on the scanned area where ammonium hydroxide is the source

Table 3.1 Point spectrum test at a specified point performed on the specimen

Element	**Atomic Number**	**Series**	**norm. C [wt. %]**	**Atom. C [at. %]**	**(1 Sigma) [wt. %]**
Oxygen	8	K-series	33.33	31.32	3.37
Carbon	6	K-series	43.94	55.01	4.47
Sulfur	16	K-series	1025	4.81	0.33
Aluminum	13	K-series	8.78	4.89	0.38
Nitrogen	7	K-series	3.70	3.97	0.66
		Total	**100.00**	**100.00**	

4. Experimental Setup

The CNTRENE^{TM} 3021 B3-R solution, which is specially designed for spin and spray coating applications, is obtained from Brewer Science. Per specifications, the average length of the CNTs is approximately 0.4 µm to 0.6 µm. Although spray coating would be a preferable process for large scale applications, spin coating is used to form a thin CNT layer on a transparent glass substrate with smaller dimensions or coating area. For this research purpose, the Chemat KW-4A spin coater was used, shown in Figure 4.1.The spin coating method will provide a thin uniform layer of coating. The thickness of each layer is controlled by the applied RPM, time of spinning, and the operating temperature. The thickness of the layer is inversely proportional to the rotation speed of the spin coater. For example, a thin layer is achieved by very high revolution per minute. At low revolution per minute, the thickness will be high for the same operating time. The research will show how the CNTRENE^{TM} solution will be used to deposit a layer of CNTs on glass, creating a transparent and heating prototype.

Figure 4.1 A Chemat KW-4A spin coater is used to perform the modified static dispense spin coating (Chemat Scientific Equipment, 2010)

For this experiment, a one-sided adhesive copper tape was used as an electrode, and was placed at the opposite edges of the CNT-coated transparent glass. A multi-meter was used to measure the resistance of each specimen. The optical transmittance of each specimen was measured by using an Evolution^{TM} 260 Bio UV-Visible spectrophotometer. An FLIR thermal imaging camera that has a spectral range of 7.5 µm to 14 µm is used to capture the temperature distribution on the surface of the specimen. FLIR ResearchIR Max software was the user interface for active thermography and also used as a data acquisition system.

4.1. Spin Coating

The slide was examined closely for any sort of imperfection such as small scratches and pits. The slide was then treated with ethanol to get rid of atmospheric dust and fingerprints. The ethanol treatment provided better adhesion between the glass and CNTs, even though the CNTs had self-interconnections and self-adhering capabilities. The ethanol-treated slide was then loaded into the spin coater chunk where the glass slide was held rigidly using a vacuum suction technique. The CNTRENE^{TM} was applied on the entire surface of the transparent glass. To obtain stable uniform coating, the solution was allowed to stay on the top of the glass substrate for 30 seconds. The pipette was positioned at an angle of 45 degrees for an increased level of visibility and dispersion rate. A quick spin of 2000 RPM was applied for 30 seconds to get rid of excess coating material.

For this spin coating process, a modified static dispense coating mechanism was used, which resulted in the uniform coating. Additional layers were obtained by repeating the spin coating procedure without cleaning with ethanol. Each layer was allowed to dry for five minutes under atmospheric condition before coating another layer, as the solution

was highly evaporative. Different stages of solution application are shown in Figure 4.2.

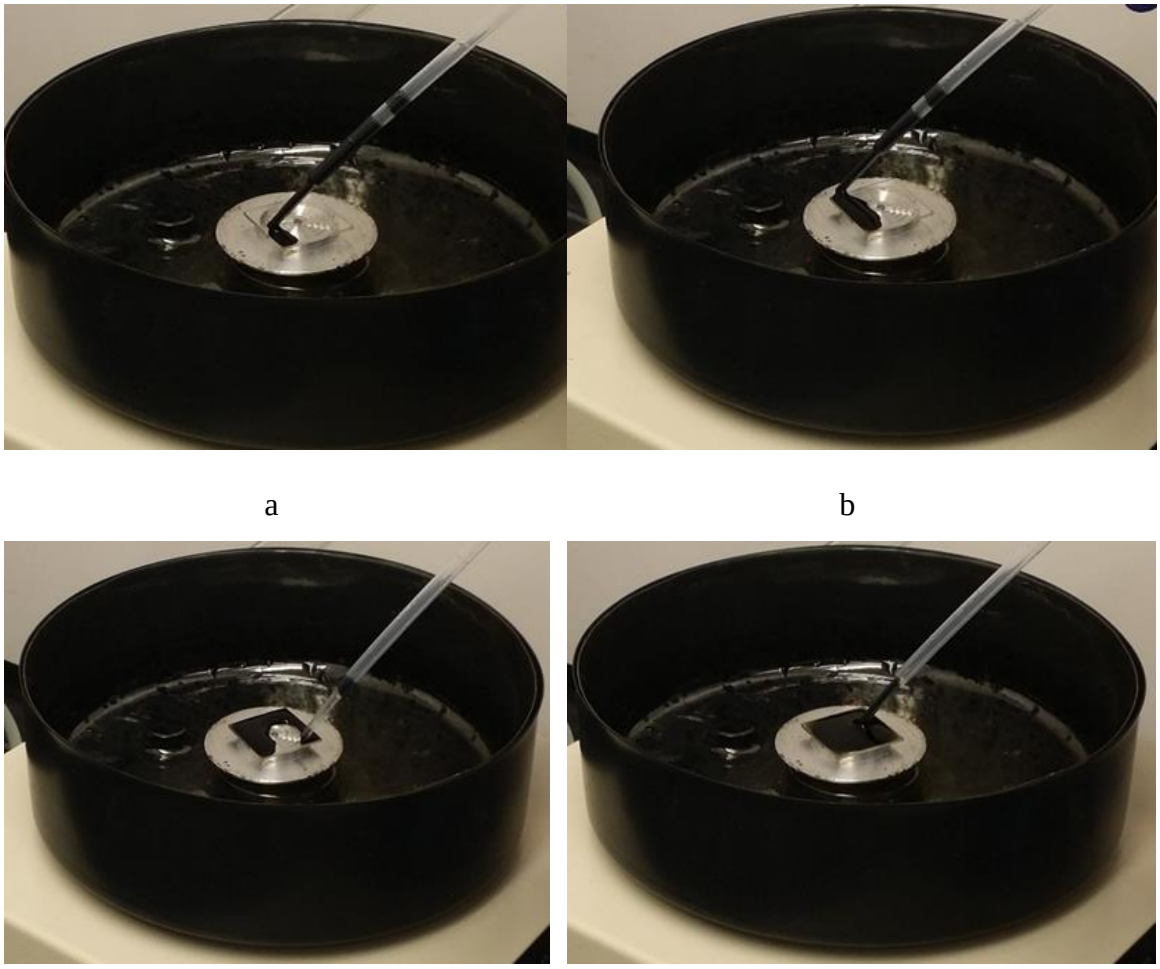

a b

c d

Figure 4.2 Different stages of CNTRENE™ deposition on the substrate at the angle of 45°

4.2. Procedure for Testing Heater Performance

DC power was generated by two 48 V DC power sources which were connected in series. It also had the capability to measure the resistance and current for the applied voltage. This power source was directly connected to both ends of the copper electrodes. The current and resistance were measured digitally in ampere and kilo-ohms respectively. The complete electrical setup is shown in Figure 4.3.

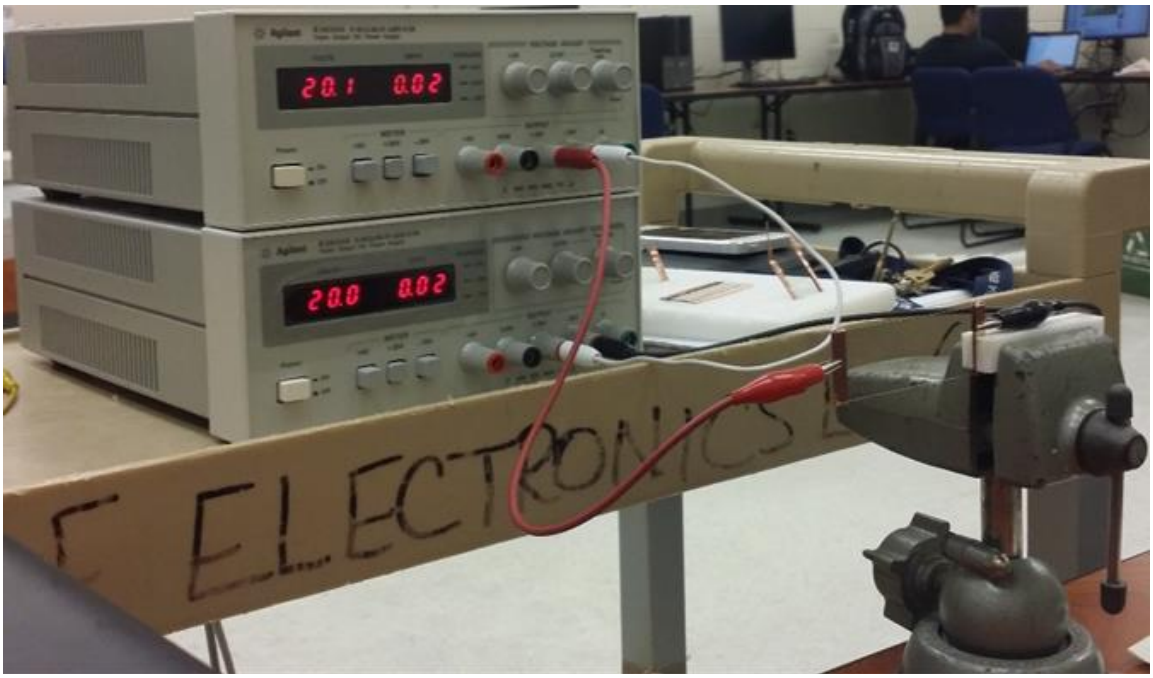

Figure 4.3 Electric circuit setup to apply DC voltage on the electrodes

The FLIR thermal camera was used to capture the temperature of the coated side. For the applied voltage, the surface temperature emitted by the CNT coating was measured. The camera needs to be calibrated with an emissivity value for the materials being studied. The emissivity was chosen as 0.95 because a study found that CNTs are a near perfect optical absorption material and generally the emissivity ranges from 0.91 – 0.95 with respect to the temperature range (-40 °C to 300 °C) for this research (Yoon, Song, Hong and Han, 2007). Also, the temperature readings were verified with the digital thermometer by performing a surface contact method. Figure 4.4 shows the thermal image of the specimen where the emissivity is fixed to 0.95. As the carbon nanotubes have a darker-colored surface, the emissivity value observed was close to 1. In comparison, the copper electrodes have a shiny surface, which provides an emissivity value observed closer to 0. Infrared thermal image obtained by the FLIR thermal camera shows the temperature distribution profile where the temperature scale is given in Celsius, as shown in Figure 4.5.

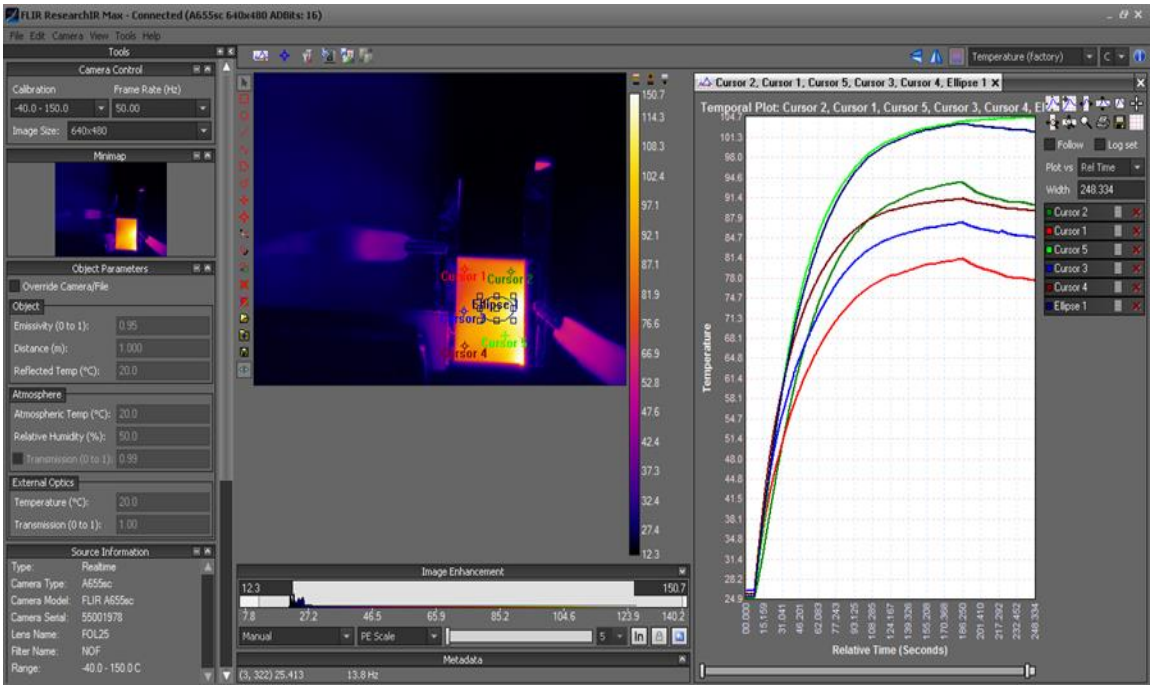

Figure 4.4. Screenshot image of FLIR Research IR Max software interface for data acquisition

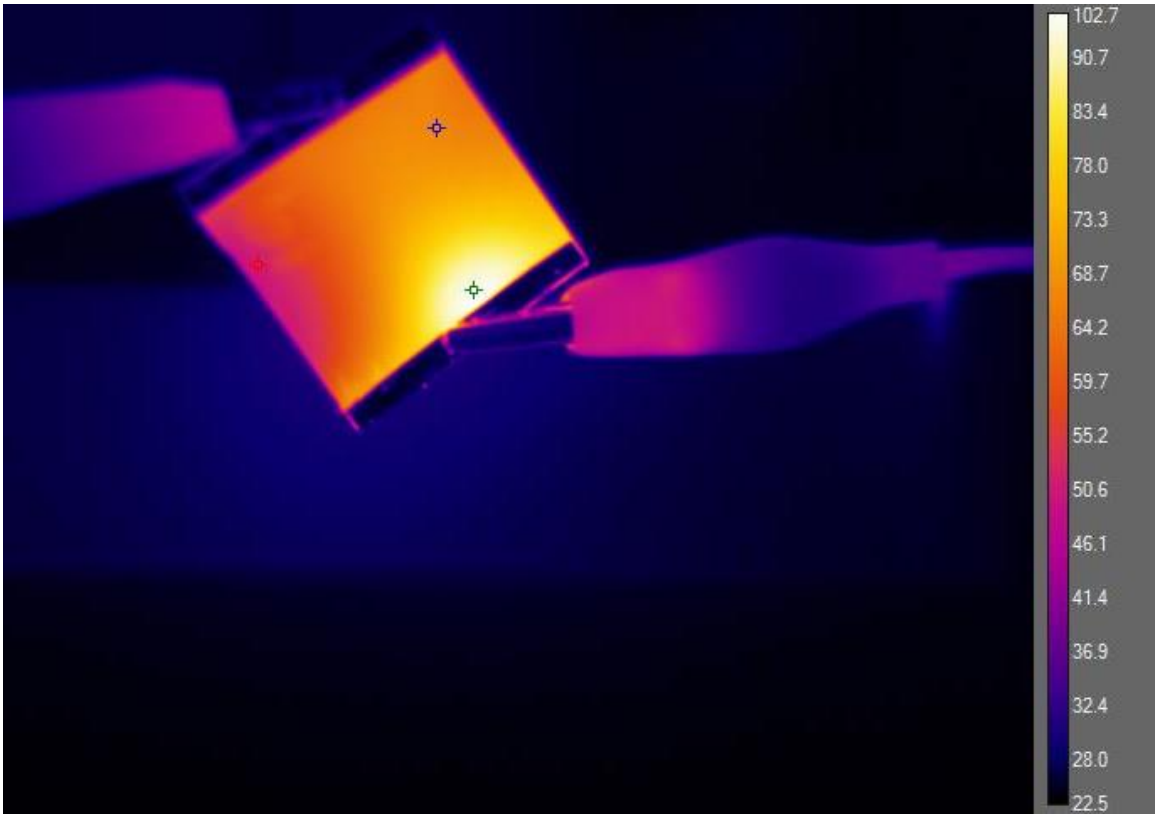

Figure 4.5 Infrared thermal image obtained by FLIR thermal camera shows the temperature distribution profile where the temperature scale is given in Celsius

5. Results and Discussion

5.1. Performance of Transparent Film Heater

Glass slides uniformly coated with CNTRENE^{TM} showed a satisfactory electrical resistance. A typical five-layer CNTRENE^{TM} coated transparent glass heater had a sheet resistance of 3.5 KΩ to 4.5 KΩ and a transmittance of 93%. A nine-layer CNTRENE^{TM}-coated transparent glass has a sheet resistance of 1.3 KΩ and a transmittance of 88%. It was observed that increasing the number of layers increases the time to reach peak temperature for the same applied voltage. Also, the resistance decreases with the increase in the number of CNTRENE^{TM} layers, but it was observed that, after four layers, there was no significant reduction in resistance, as shown in Figure 5.1. All slides used in this figure had a coated area of 5 cm^2.

It is well known that the electrical resistance of any conductive material (such as CNTs) is strongly based upon the operating temperature (Barberio, Camarca and Xu, 2007). The experiment showed that the resistance decreased initially with an increasing temperature. This was due to the negative thermal coefficient (NTC) effect. Due to the NTC effect, the specimen increased its temperature rapidly as the voltage was applied. This was due to an initial higher resistance. The NTC is commonly observed in elements such as carbon, silicon, and germanium. Figure 5.2 shows the NTC effect where the initial resistance was high and then dropped before increasing with the increase in temperature.

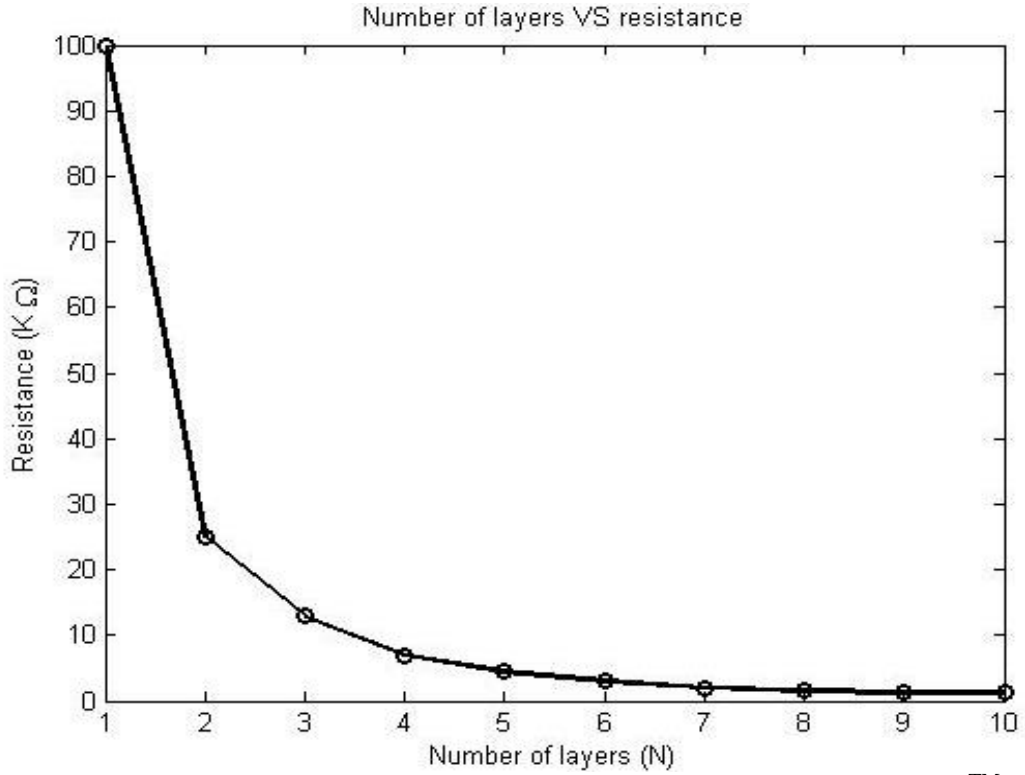

Figure 5.1 The resistance decreases with an increasing number of CNTRENE™ layers

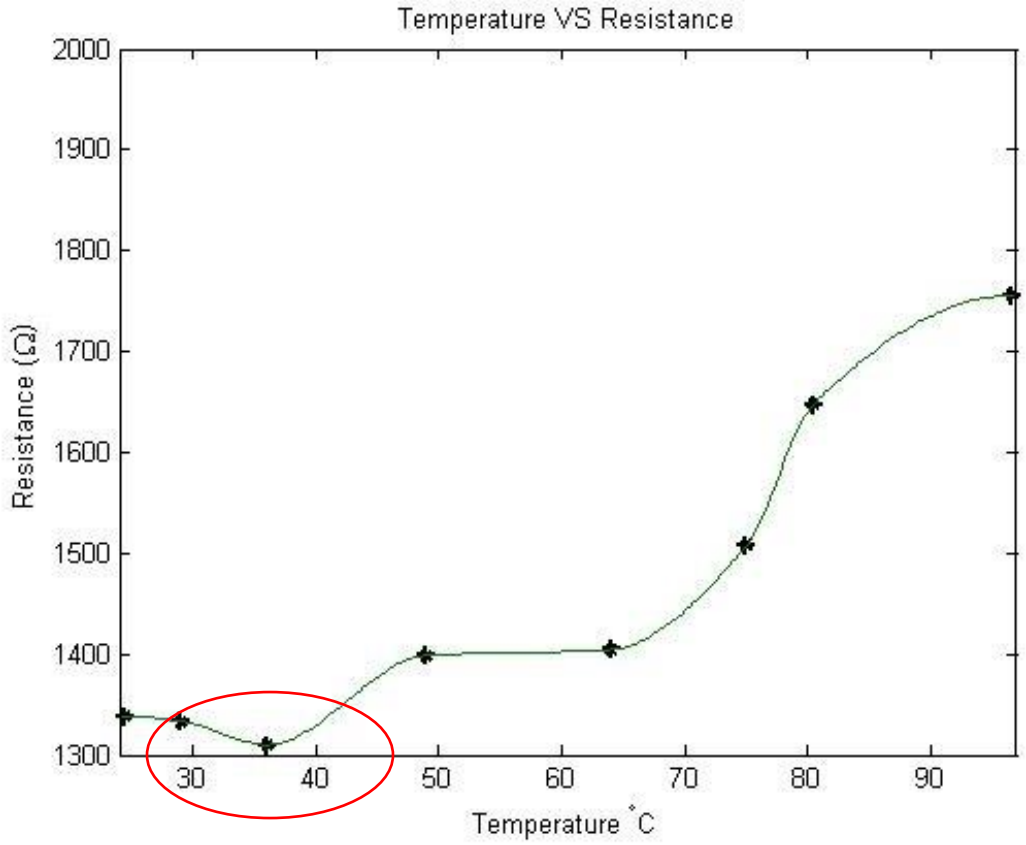

Figure 5.2 Observation of Negative Thermal Coefficient (NTC)

5.2. Transmittance

A UV-visible spectrophotometer was used to perform the transmittance test on the CNTRENE^{TM}-coated transparent glass specimen. The spectrophotometer was calibrated to 100% transmittance for an uncoated glass slide. The wavelength ranged from 350 nm to 800 nm, which is the visible wavelength spectrum. All glass specimen showed an optical transmittance of above 85%. As per most state laws, a typical car windshield should maintain the transmittance of 70% or above. Transmittance decreases with an increase in the number of CNTRENE^{TM} layers, as shown in Figure 5.3. The variation of transmittance with number of coatings is tabulated in Table 5.1.

Table 5.1 Variation of transmittance with number of coatings

Slide Number	Number of Coatings	%Transmittance
11	1	98
12	2	96
16	2	97
20	2	97
13	3	95
17	3	96
21	3	95
14	4	94
18	4	94
22	4	94
15	5	93
19	5	93

23	5	92
24	5	93
25	5	92
26	6	92
27	7	91
28	8	88
29	9	87
30	10	86

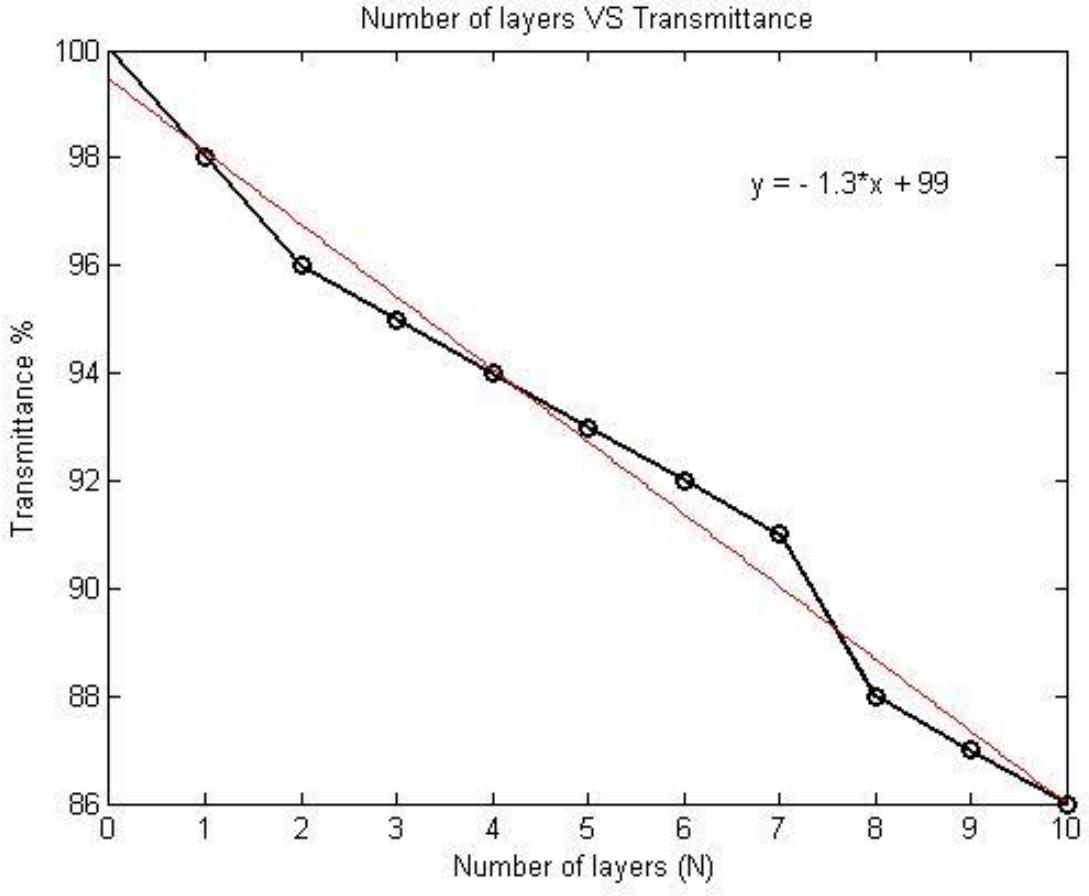

Figure 5.3 Transmittance decreases with an increasing of number of CNTRENE^{TM} layers

5.3. Temperature vs Time Profile

FLIR ResearchIR Max software was used for data acquisition. By using the software, a constant line of data collection points was created on the specimen to collect a significant amount of data. The applied voltage was regulated from 0 to 120 V and it was observed that the surface temperature increased immediately upon application of the voltage. A five-layer specimen reached a peak temperature of 85°C and a nine-layer specimen reached 101°C in less than two minutes.

A continuous cycle performance test was performed on a five-layer sample. A voltage of 80 V is applied, then turned off manually before being applied again for ten successive cycles. The goal of this test was to reach 60 °C from 30 °C. For this experiment the emissivity was set to 0.95 and the transmittance was set to 1, as the carbon nanotube side faced towards the infrared camera. The fast heating and cooling response was observed and there was no degradation in performance observed during the test. An average cycle took 210 seconds to reach from 30 °C to 60 °C and back down to 30 °C. Also, it was observed that all cycles follow the same pattern of heating and cooling. All the data points were extracted from the software by using web plot digitizer, as the software user interface had limited capability to generate the graph. The extracted data was used to generate the plot using MATLAB. Also, these data points were used for future interpretation. Figure 5.4 shows the continuous cycle test results obtained using the FLIR Research IR MAX software.

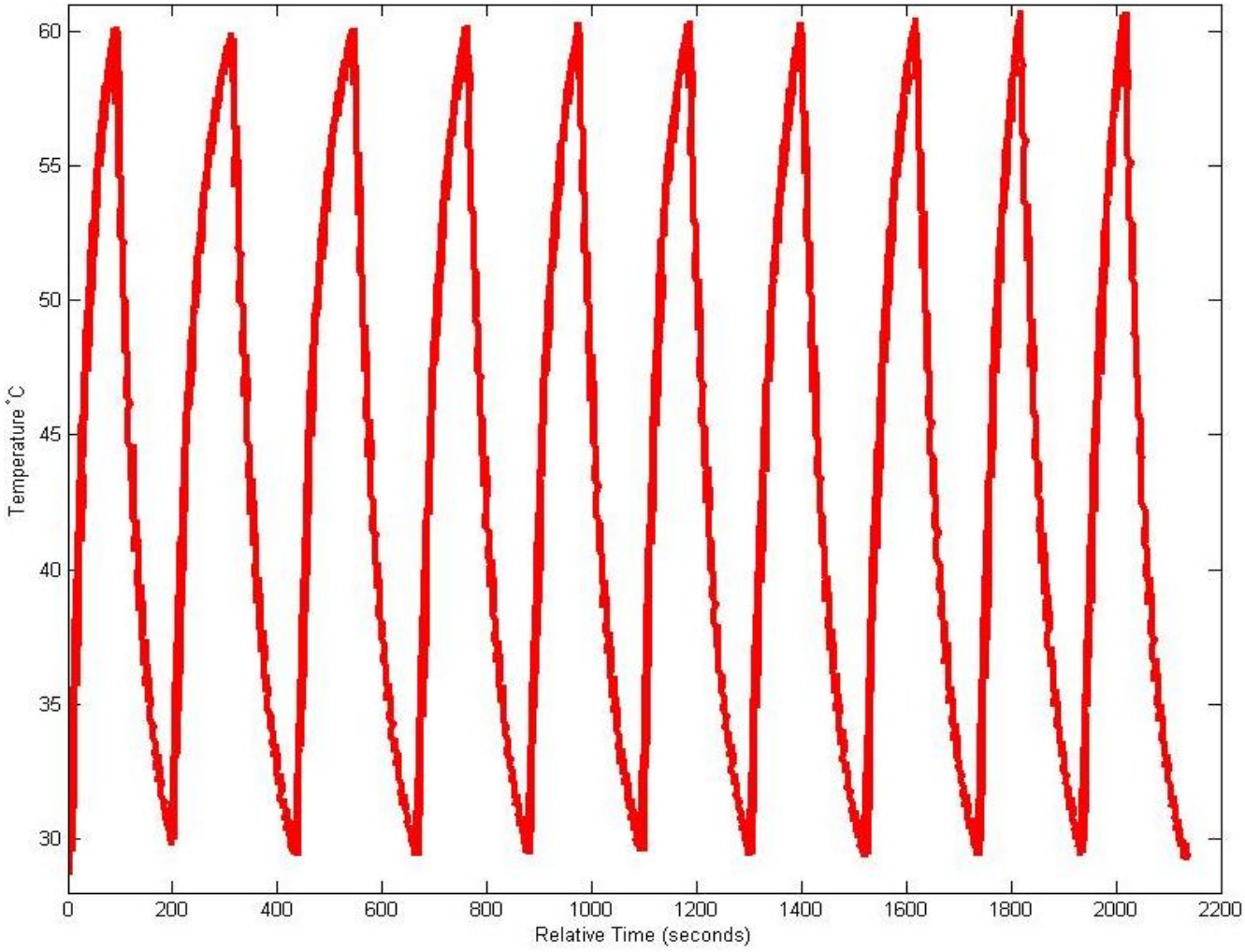

Figure 5.4 Continuous cycle test results which is performed with FLIR Research IR MAX software.

5.4. Thickness vs Temperature profile

The heating performance mostly depends upon the thickness of the carbon nanotube layer formed on the surface of the specimen. We attempted to measure the thickness using the Quanta 650 scanning electron microscope. It was found that measuring the thickness of the carbon nanotube coating was time consuming, because it was very difficult to align the specimen at the angle of 90 degree or parallel to the electron beam source. In order to achieve the perfect angle the stage was rotated or tilted. The procedure was repeated to measure the thickness of four-layer, six-layer and seven-layer samples. However, the measured thickness was determined not to be accurate due to the difficulties in

measurement. Moreover, as CNTRENE^{TM} solution had run off the slide, it was difficult to see where the slide ended and the coating began.

However, it was observed that the thickness of the coatings varied throughout the length at the microscale. This would result in a somewhat non-uniform coating, which could account for some of the temperature variations reported later. Due to the difficulty in measuring the thickness of the layers, there is unfortunately no quantitative data to report.

To support that the thickness could impact or alter the performance, the temperature profile was recorded for specimens with different numbers of layers. A constant voltage of 120 V was applied and the temperature plot was generated with respect to time in seconds as shown in Figure 5.5.

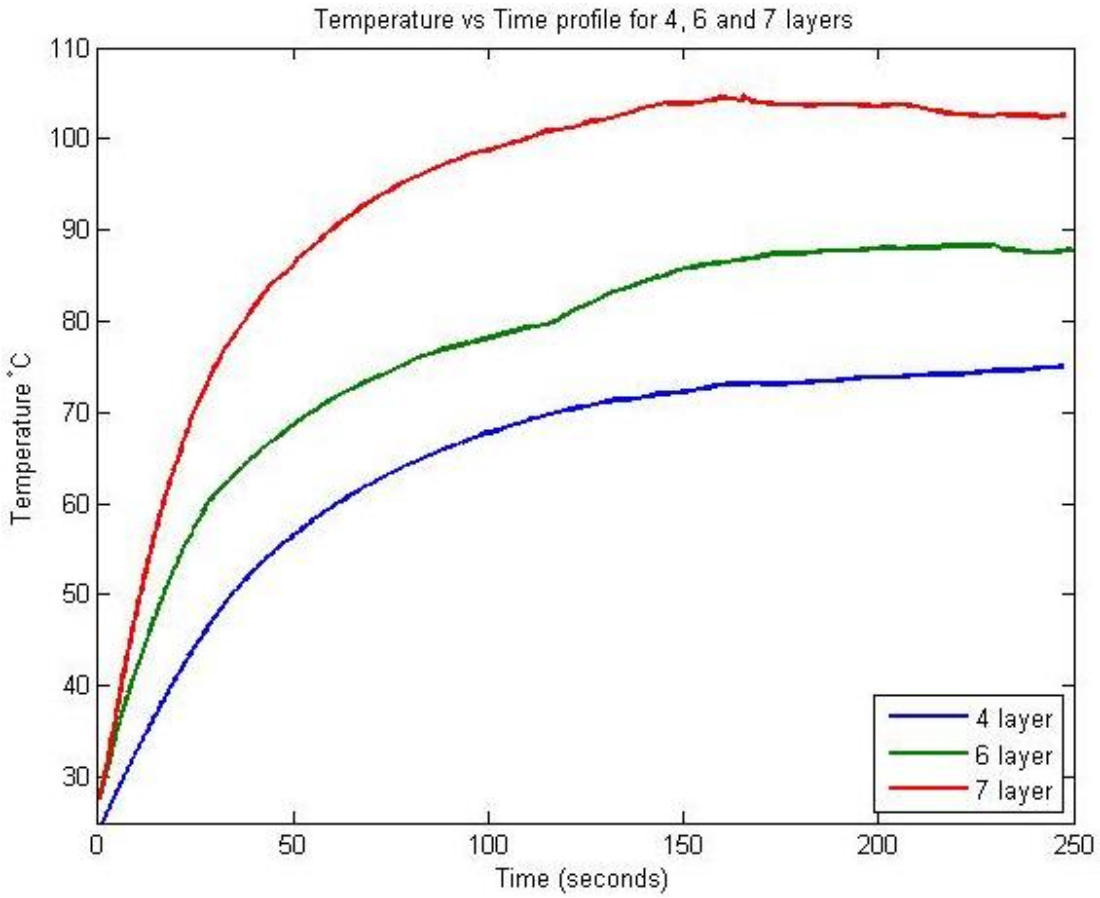

Figure 5.5 The temperature plot for different layers sample with respect to time for the applied 120 V

5.5. Stability

A weekly lifetime performance test was performed on two 5-layer slides and one 9-layer slide for nine weeks. Figure 5.6 shows the life-time test performed on three slides under the constant voltage of 80 V. It shows the average temperature 75 °C and 115 °C for the five-layer and nine-layer slides, respectively. To avoid lifetime degradation, the slide was coated with a protective coating. This coating isolated the CNTRENE^{TM} layers from atmospheric contact, which was also done by sandwiching, or protective inert coating, or applying high performance thermal tape, as described later.

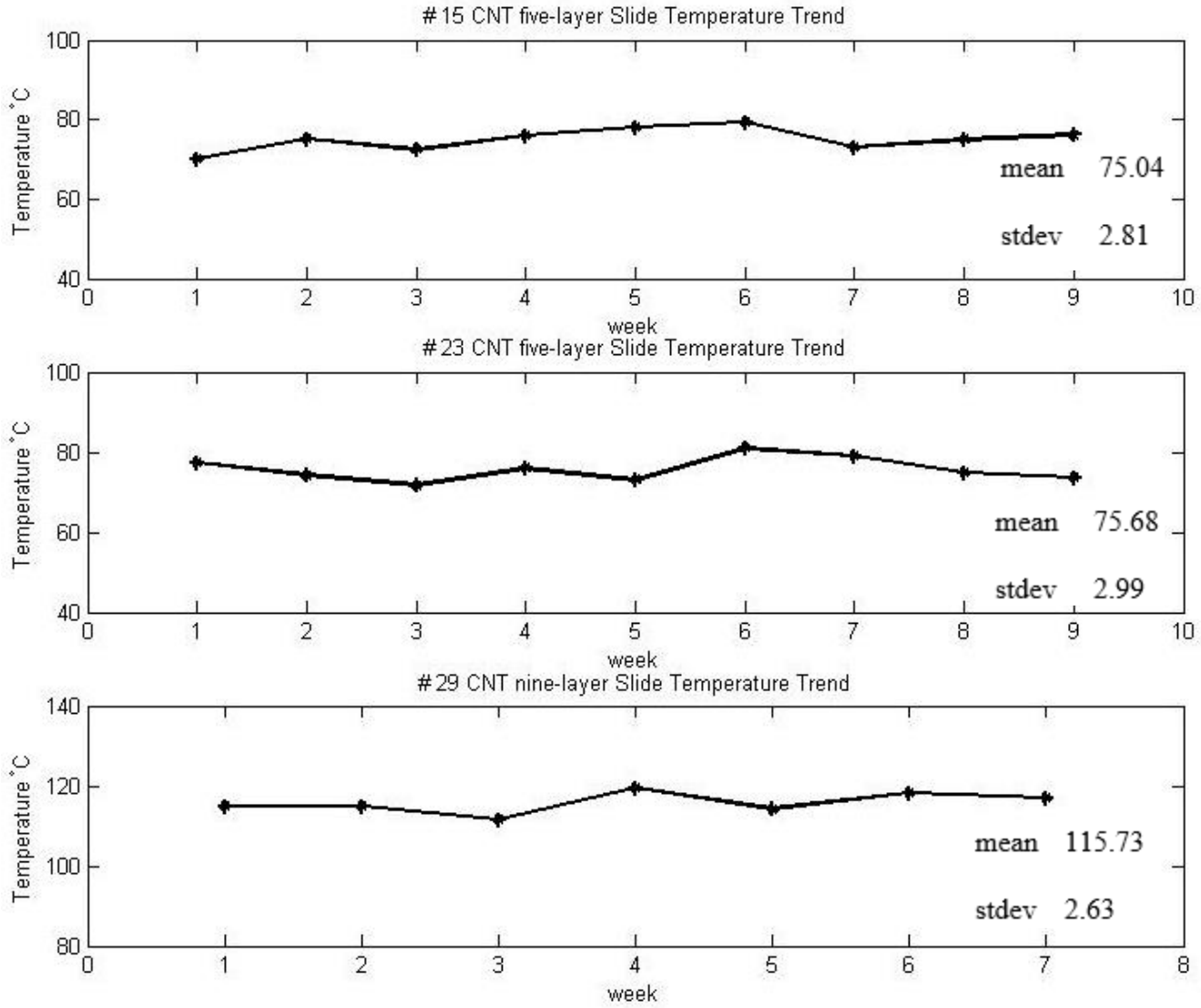

Figure 5.6 Lifetime performance test for three different samples

5.6. Repeatability

The repeatability of the experiment was tested on different samples. All of the samples produced the same output as the parent sample. The test was conducted on a total of 50 samples. The samples included microscope slides, annealed glasses, laminated glasses, and tempered glasses, which are used to manufacture actual car windshields. Regardless of the glass sample, each specific carbon nanotube coating generated the same resistance output along with transmittance and other general properties.

5.7. Power Requirements

The governing equation to determine the total power consumption (P) for operating the transparent heater is written as

$$P = V\,I \tag{1}$$

where V is the voltage applied and I is the current. The heat generated by the heater is dissipated into the atmosphere in terms of conduction, convection, and radiation. Convection and radiation were not taken into account as the specimen was not in contact with any object except air. Hence, the heat generation was measured in terms of conduction by using the thermal camera. The surface power density is calculated by

$$\mathrm{P}_d = {}^{P}\!/_{A} \tag{2}$$

where A is the CNTRENE^{TM} coated surface area (ignoring the area covered by electrodes). To test the repeatability and scalability, two specimens with different dimensions are used. The total dimensions are 25 × 25 mm and 25 × 50 mm and the CNTRENE^{TM}-coated areas are 5 cm^2 and 10 cm^2, respectively. The goal is to calculate the surface power density. For this we have to measure the voltage required to reach 70 °C for both samples. The power requirement is calculated by using Eq. (1). For the 25 × 25 mm and 25 × 50 mm slides, the

voltage requirement to reach 70 °C is 60 V and 80 V respectively. This voltage is then multiplied by the measured current (0.02 A and 0.03 A respectively) to obtain the power. The surface power density is calculated by using Eq. (2) as 0.24 watts/cm^2 for both samples. This value is only indicative, as some non-uniformity in the temperature distribution over the coated area was observed.

From the above calculation, for a typical five layer CNTRENE^{TM}-coated specimen with same manufacturing parameters, the surface power density is 0.24 watts/cm^2. This experiment has proven that similar manufacturing parameters have produced specimen with same surface power density, regardless of surface area. Once the power density is determined for the specific manufacturing parameters, it is possible to find the input voltage requirement prior to manufacturing with respect to area.

5.8. Ice and Mist Detachment Test

The goal of the experiment was to determine the time required to detach a layer of ice from the transparent heater surface. To detach the ice from any surface, it was important to break the surface contact between the ice and the surface. The prototype specimens were loaded into the freezer unit. On the surface of the specimen, droplets of clean water were placed, which covered approximately 50 percent of the surface area. The freezer unit was set at maximum cooling to convert the water droplets into ice. After 2 hours the specimen with ice is taken out and kept at room temperature, as shown in Figure 5.7.

The specimen was held at a 45 degree angle to simulate an actual windshield setup. Immediately after the setup, a voltage of 120 volts was applied and the time was recorded. After a few seconds the ice detached from the surface and fell off. On the other hand, the specimen at room temperature without any external force took more than 3 minutes to

detach the ice from the surface. Consecutive experiments are done with the same setup and the time was tabulated, as shown in Table 5.2.

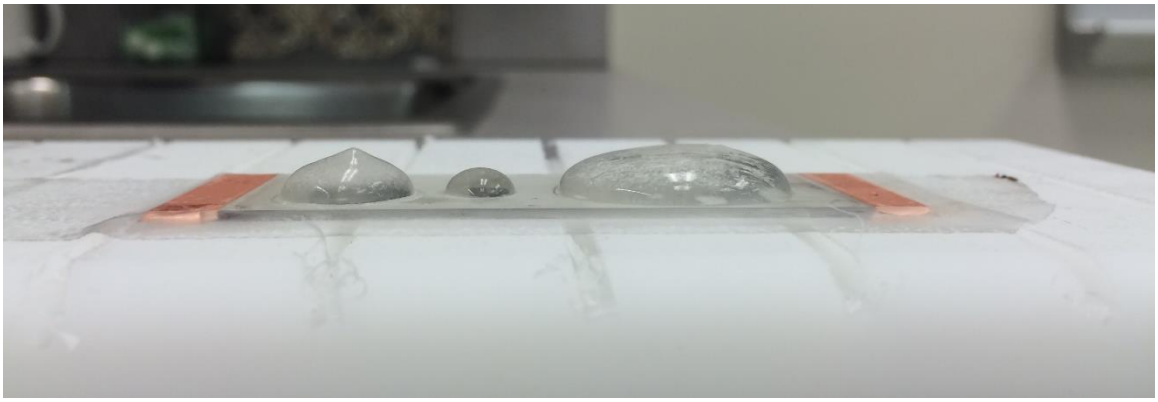

Figure 5.7 The specimen with ice is taken out and kept at room temperature to perform detachment test

Table 5.2 Time taken to detach the ice from the surface

Experiment Number	**With Voltage (seconds)**	**Without Voltage (seconds)**
1	4.3	190
2	4.7	205
3	4.3	187
4	4.2	191
5	4.6	201

6. Protective methods

To avoid performance degradation during long term usage it is necessary to protect the carbon nanotubes from oxidation because CNTs degrade at high temperature. This can be achieved by using a non-reacting or inert type protective coating.

6.1. Sandwich Composite

The first possibility that was investigated was an acrylic transparent conformal coating 1-µm thick as it was thought it would be the most suitable for our application. This coating fulfills the transparency, temperature stability, and compatibility requirements for retaining the CNTRENE^{TM} properties. The coating was applied in an isolated environment. The coated specimen was allowed to cure for five minutes under an ambient environment. This coated specimen was sandwiched by using a transparent adhesive applied with an edge adhesive technique. This isolated the carbon nanotubes from environment disturbance without losing the optical transmittance. For this, DP 460 off-white epoxy adhesive was used, which is a high-performance adhesive. Also, DP 460 has very high shear strength and was used to provide very high resistance against water penetration and to obtain the sandwiched structure.

To perform edge adhesion, the base and accelerator were mixed in the ratio of 2:1 for five minutes. The mixed adhesive was allowed to set at room temperature for another 15 minutes. This process removed the cloudiness and micro air bubbles from the adhesive. Also, it increased the viscosity of the epoxy adhesive. The bubble free adhesive was applied on the edge of the sandwich composite. The prepared sample was allowed to set for 24 hours at room temperature.

The water penetration test was performed on the prepared sample for 48 hours, as shown in Figure 6.1. This test was a standard method for field determination under uniform pressure load and it was found that there was no water penetration.

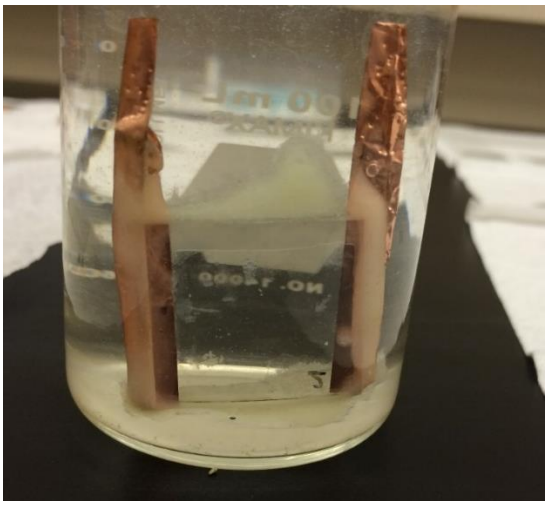

Figure 6.1 Sandwiched structure under water penetration test

Once the water penetration test was finished, no water was visually observed in the sandwich structure. Also, the transmittance was found to be the same before and after testing. By sandwiching the CNT layer, another layer of glass was introduced between the carbon nanotube coating and the thermal camera. So, to get accurate results, the transmittance value was changed in the thermography software. This will neglect the conduction issue with the sandwiched glass. The water-tested specimen is shown in Figure 6.2. Then, the sample was tested by applying the voltage and unfortunately, the current consumption had dropped, showing that the overall performance had been reduced drastically. It was found that the applied adhesives disturbed the carbon nanotubes around the edges. The adhesive flowed between the sandwiched layers and disturbed or eliminated the carbon nanotube coating around the edges. These carbon nanotubes were the main contributors for providing the continuous channel arrangement which also act as a bridge for the carbon nanotubes at the center of the glass. This, in turn, showed that the performance was compromised.

Figure 6.2 Sandwiched structure after water penetration test shows there is no water was visually observed

6.2. Protective Inert Coating

Since a performance drop had occurred during the sandwiching method, another way of isolation method was needed. Protective coating was an alternative method. This protective coating was achieved by spraying a special transparent, non-reactive inert aerosol spray.

In selecting a spray, it is necessary that it does not react with the carbon nanotubes on the surface of the substrate. The spray should be a perfect insulator and withstand the operating temperature. Also, it should not react with water, foreign objects, and any other solvents. To match these requirements, a special non-reactive acrylic aerosol spray was chosen, manufactured by Electrolube Inc. The spraying of the protective coating was achieved in a glove box. The coated specimen was allowed to set inside the glove box for one hour. Figure 6.3 (a) shows the temperature and current output for the administered 120 V before acrylic coating was applied. Figure 6.3 (b) shows the temperature and current output for the applied 120 V after the acrylic coating was applied.

It can be clearly seen that there is a considerable drop in performance. It was calculated that the temperature drop was 16% and the current drop was 24%. This was due to a reaction that took place at the coating surface. It was also found that this reaction was unavoidable and continuous throughout the operational lifetime. Over time, this method caused the complete failure of the sample.

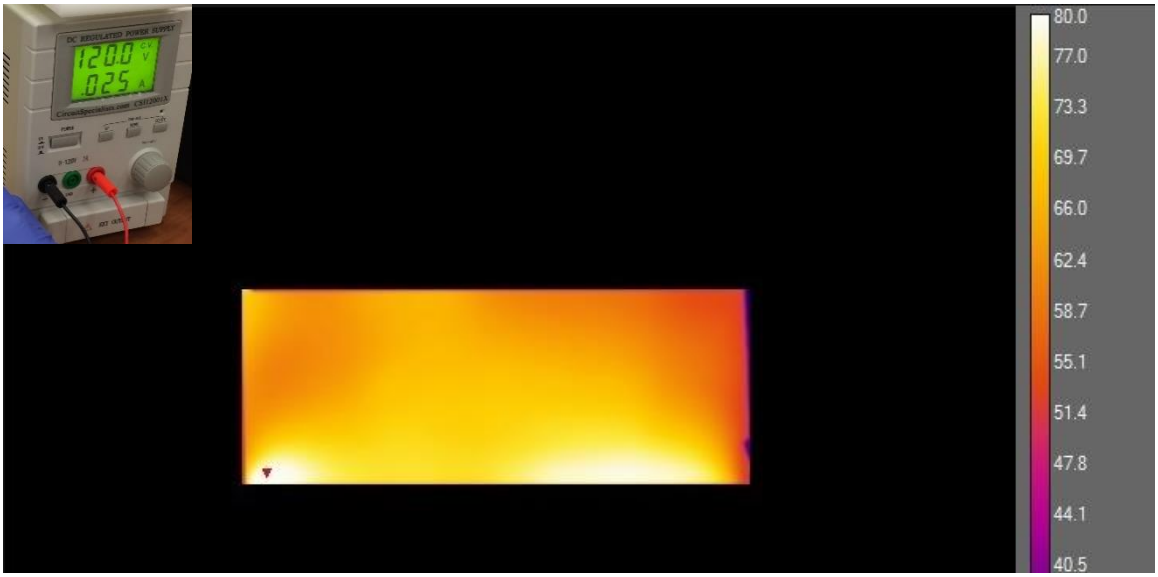

(a)

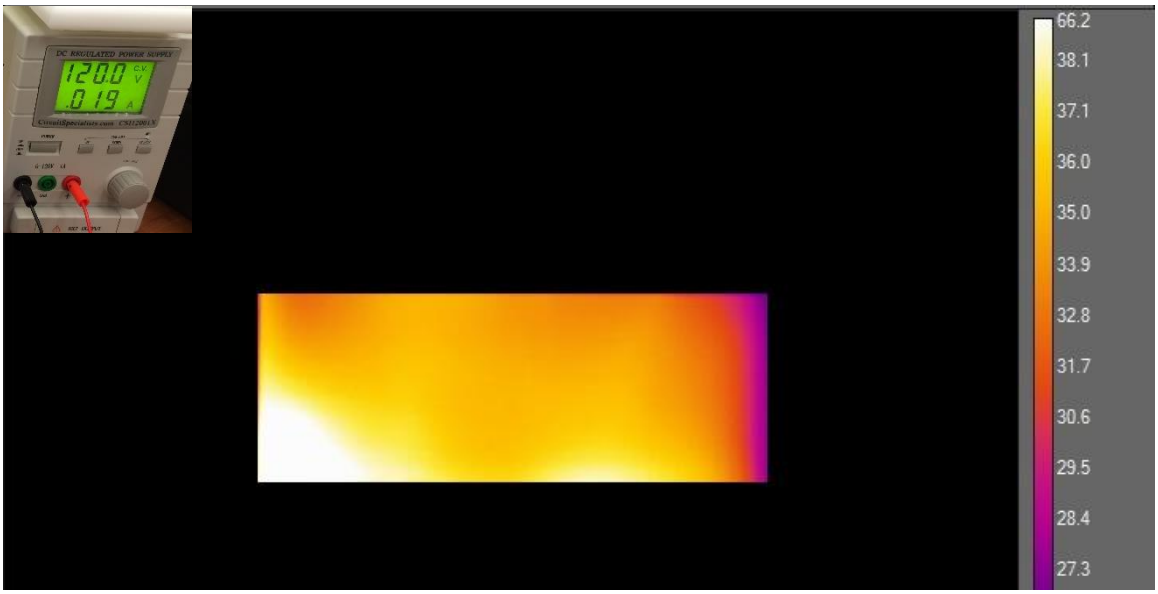

(b)

Figure 6.3 IR image and power input (a) Before (b) After the application of acrylic aerosol spray (Temperature scale in °C)

6.3. High Performance Thermal Tape

Due to unsatisfactory results, both sandwiching and protective spray coating methods were not recommended for further research. However, it was still necessary to find a new way of isolation, as the CNT layer had a good chance of losing performance when exposed to the environment. This necessity led to the perfect way of isolation, through high performance thermal tape, manufactured by 3M.

The high performance thermal tape performs two important functions. One of the functions was to protect the carbon nanotubes on the surface by creating a perfect isolation from the surrounding environment. The other function was to reduce the number of heat spots. Heat spots are zones where the temperature is far higher than the nearby areas. This was due to the presence of an increased number of carbon nanotubes on that particular zone. This is unfortunately inevitable using the spin coating method, as the thickness of the layers cannot be controlled accurately enough. Figure 6.4 show the IR image of the specimen of before and after application of high performance thermal tape, respectively.

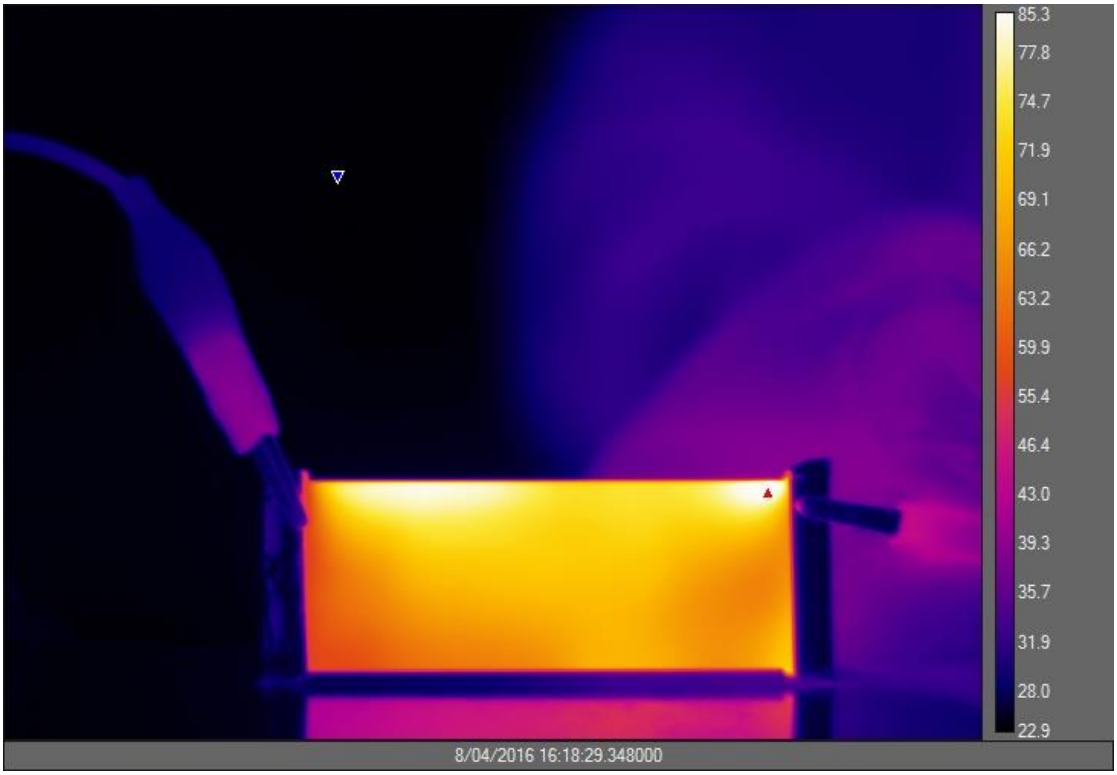

(a)

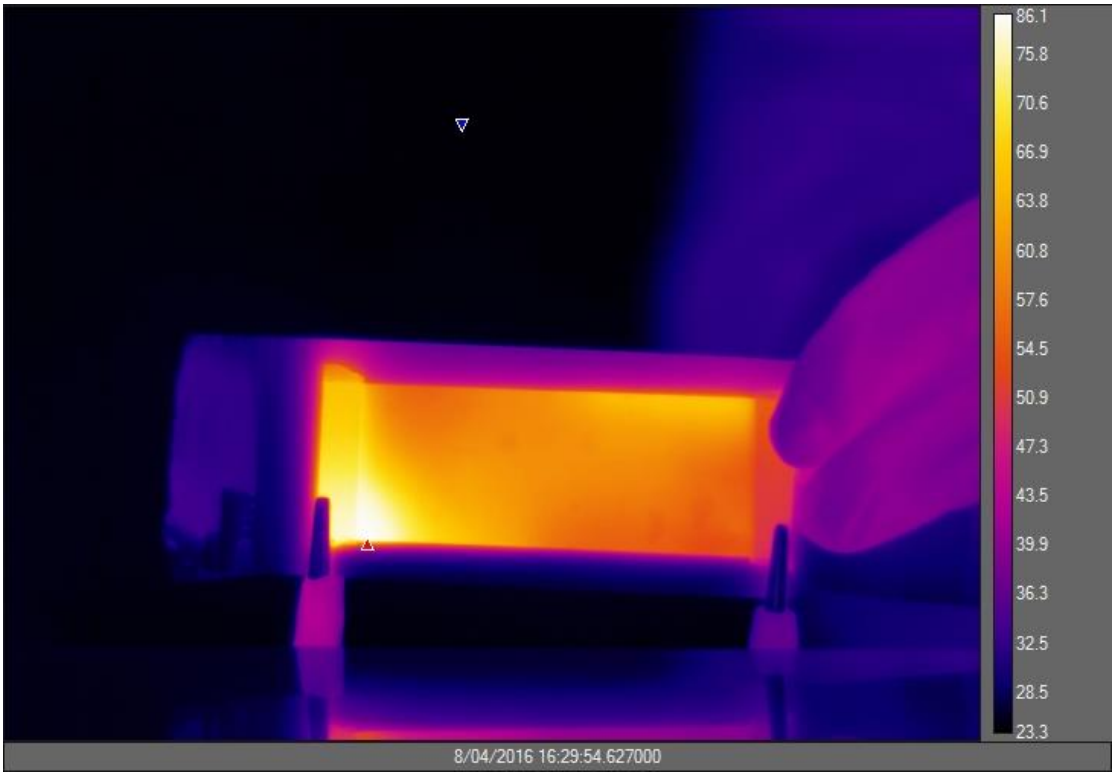

(b)

Figure 6.4 IR image – (a) Before (b) After the application of high performance thermal tape (Temperature scale in °C)

6.4. Image Processing and Contour Plots

Some of the heat spots can be seen visually, but most of them require very close examination through the post IR image processing. The maximum temperature was always attained at the contact point of the positive electrode and the minimum temperature was always attained at contact point of the negative electrode. A possible source for the difference in temperature can be attributed to the Peltier effect, which is more common in semiconductors. Other factors such as electrode/CNT layer adhesion and uniformity of the coating would also have to be considered. The Peltier effect is a thermoelectric phenomenon where some heat is transported as a thermoelectric interaction with the electrical current, in parallel to heat transport (Ari and Kribus, 2010). This process can either increase or decrease the heat flux at the contact point of the electrical circuit. In this case the contact points are electrodes. The Peltier effect is only 5% efficient in thermoelectric reactions. This Peltier effect was significantly reduced after applying the high performance thermal tape. The non-uniformity of the temperature profile clearly needs more investigation for future work.

Figure 6.5 shows the before and after images of the specimen after applying the high performance thermal tape. As explained below, the resultant image compares the before and after image, and generates the new image to show the places where the heat spot corrections and Peltier effect reductions are achieved.

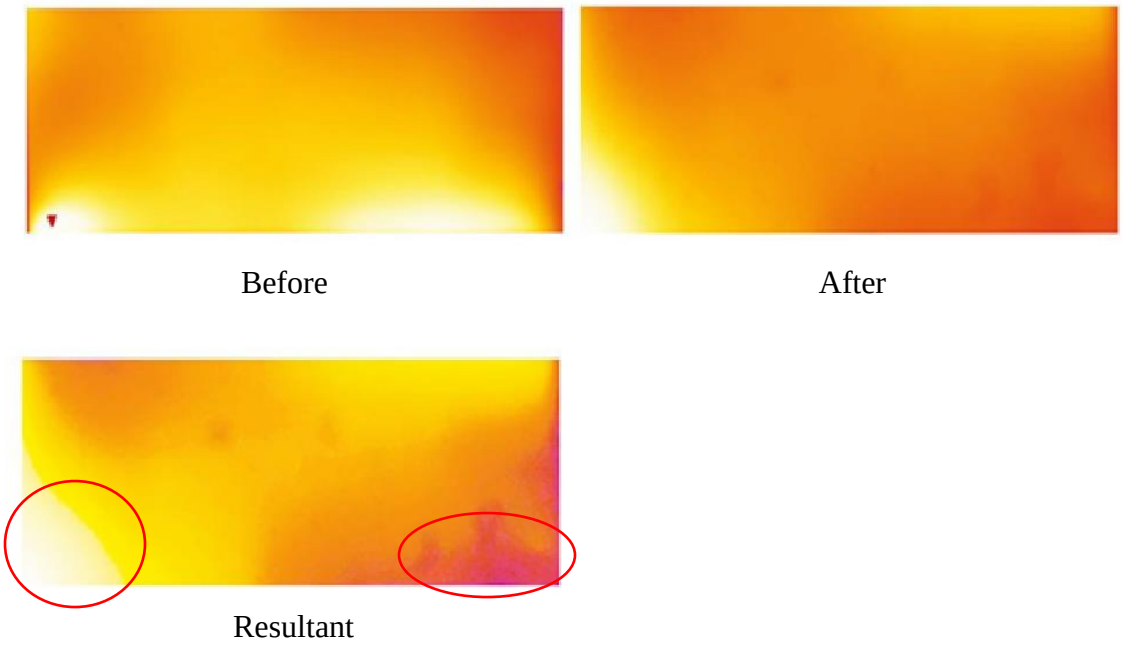

Figure 6.5 Resultant image generated after comparing the before and after image where the corrected zones are highlighted

The image processing was done by using a MATLAB image augmentation technique. This process involves reading the RGB values of the individual pixel. Two images were taken before and after applying thermal tapes, with the same number of pixels. They were then loaded into MATLAB for image processing. These images were compared with each other in pixel level for RGB values, to generate the new resultant plot based on the change in RGB value. The resultant plot showed the corrected heat spot and reduced Peltier effect. Also, each pixel value was read to plot the histogram plot. It was observed that after applying the high performance thermal tape the heat spots were reduced by 30%. Histogram plot is generated to show the effect of thermal tape, as shown in Figure 6.6.

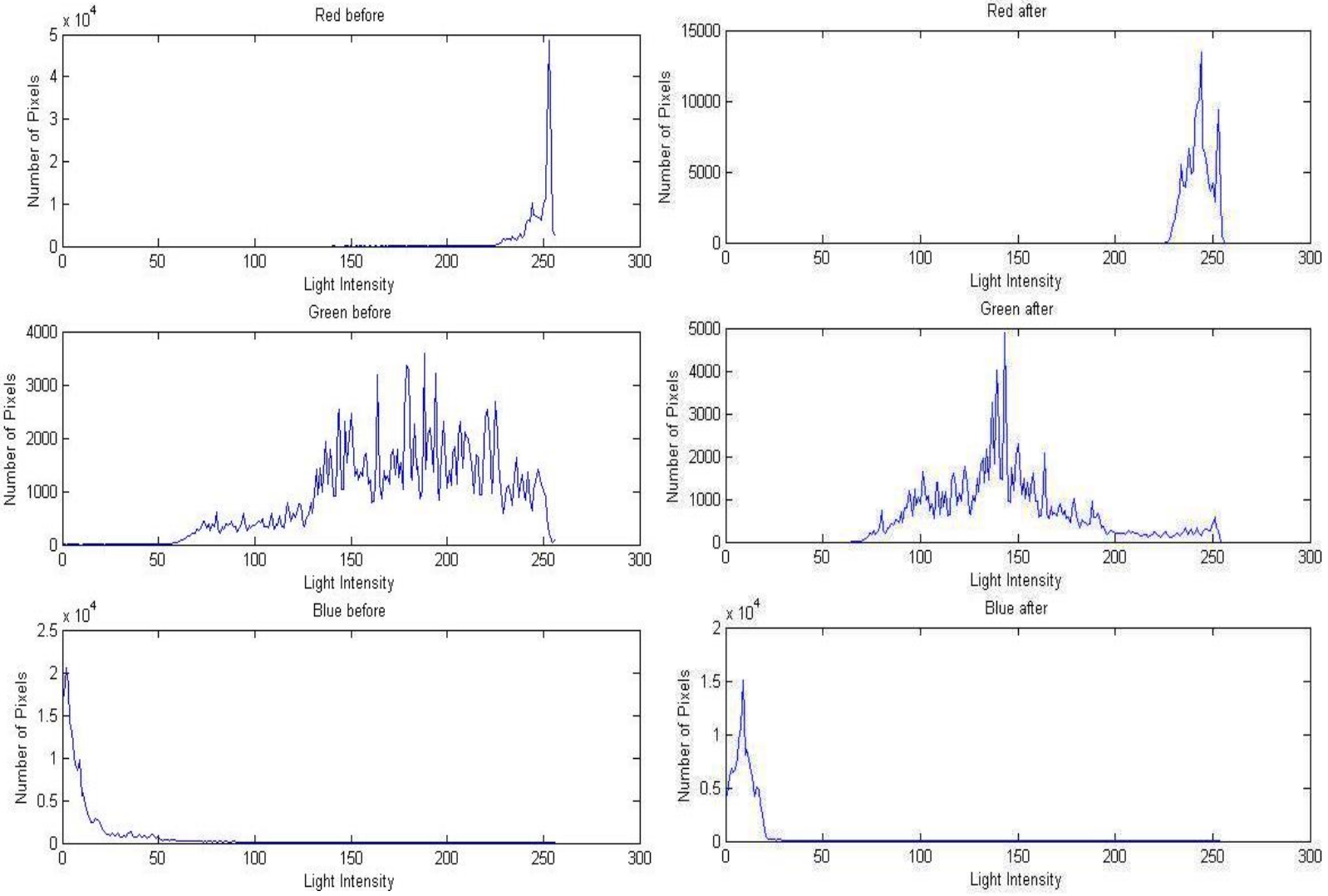

Figure 6.6 Histogram plot is generated to show the effect of thermal tape

An individual thermal contour plot was generated to show the variation or change in temperature with respect to time, on the slide with a high performance thermal tape. The temperature limit was set to 50 °C in the ResearchIR thermography software. For every 5 °C increase, the image was recorded. A step-by-step thermal image contour is shown in Figure 6.7. Also, nine data points are positioned as shown in Figure 6.7 b for data acquisition. This data was extracted with the help of web plot digitizer and the temporal plot for all nine data points, and a plot was generated by using MATLAB, as shown in Figure 6.8.

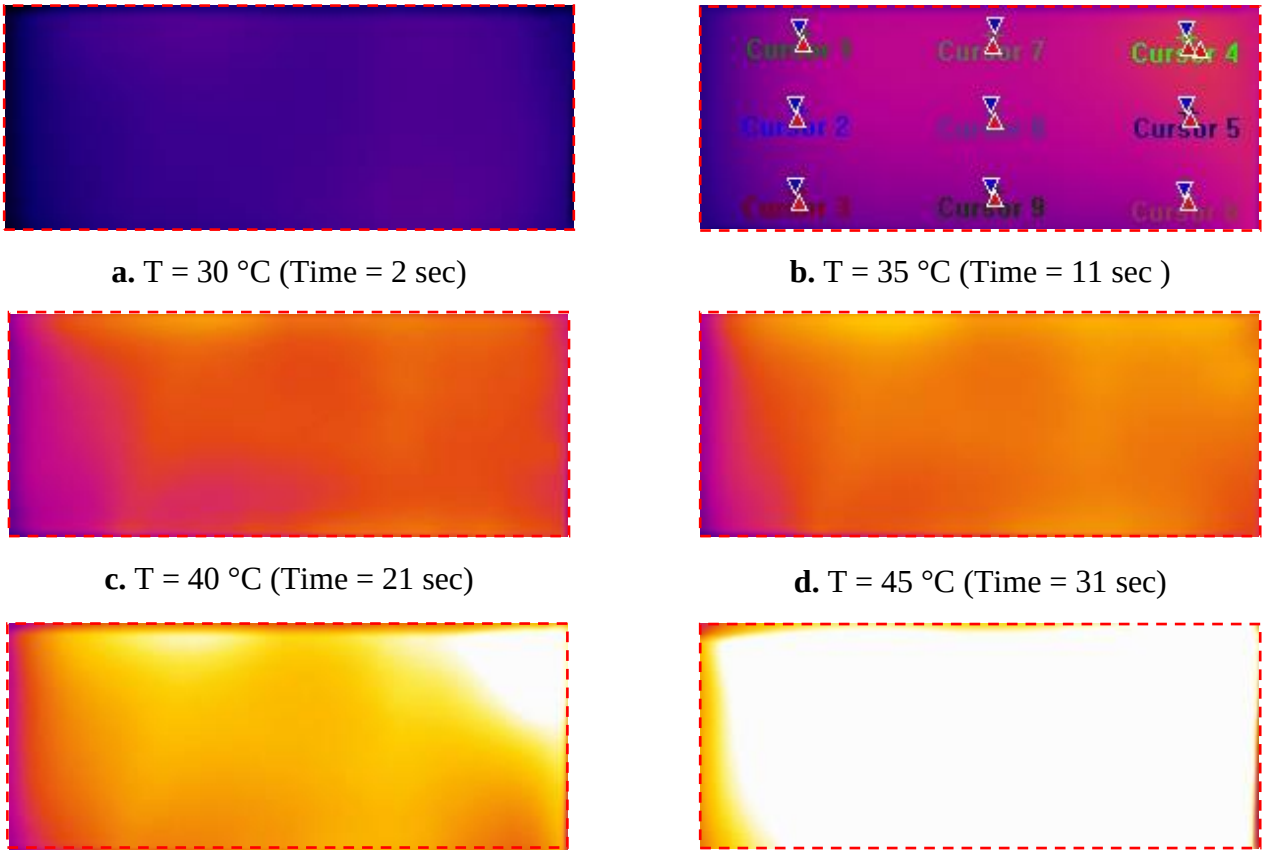

a. T = 30 °C (Time = 2 sec)

b. T = 35 °C (Time = 11 sec)

c. T = 40 °C (Time = 21 sec)

d. T = 45 °C (Time = 31 sec)

e. T = 50 °C (Time = 44 sec)

f. T >50 °C (After 50 sec)

Figure 6.7 Image contour to show the temperature variation with respect to time for the applied 120 V

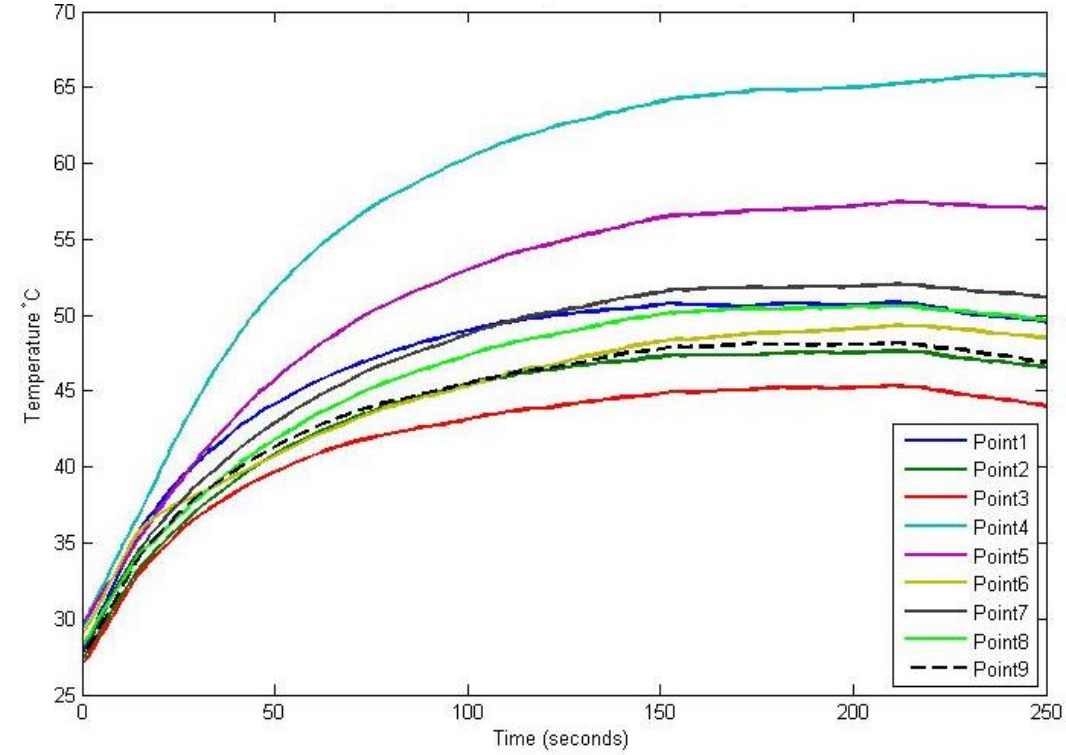

(a)

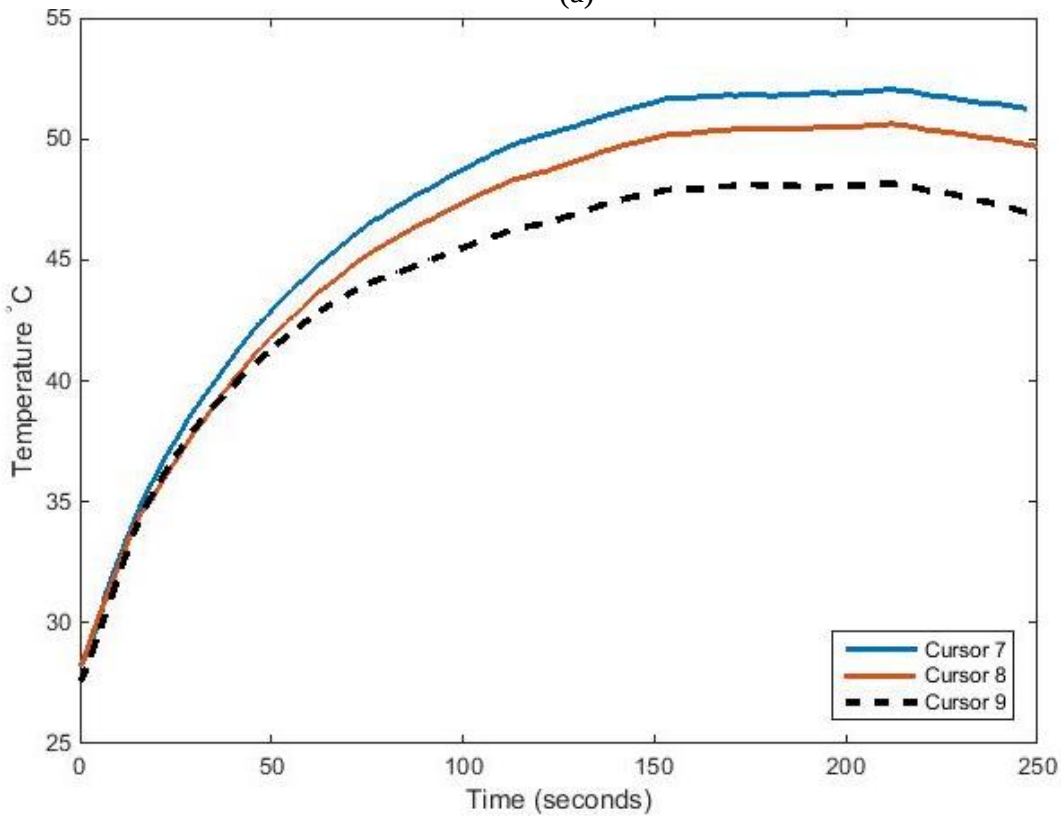

(b)

Figure 6.8 Temporal plot: (a) For all nine points and (b) For data points 7, 8, and 9 as marked in Figure 6.10 b

As the data points 4 and 5 are close to positive electrode, it experiences very high temperature and the data points 2 and 3 are close to negative electrode, it experiences very low temperature. The temperature difference between the data points is ± 5 °C, except for points 2, 3, 4 and 5, because of the Peltier effect.

6.5. Conclusion for Protective Method

From the above protective methods, it was concluded that using a high performance thermal tape could offer a superior protection for the carbon nanotube coating. This method was used to isolate the carbon nanotubes from environmental impact without losing the optical transmittance. Unlike other protective methods, the overall operating efficiency was stable throughout the operation. This protective tape comes in various colors with different level of tints that will offers privacy windows or glasses for cars/aircrafts. Also, applying this high performance thermal tape on the carbon nanotube coated surface was comparatively simpler than other methods.

7. Potential Applications

7.1. Aircraft/Car Windshield Defrost System

The above research was conducted from the idea of using carbon nanotubes for windshield defrosting and deicing. Developing a good visibility during winter time was always a crucial job for a driver or pilot to not get distracted. This can be achieved by placing a SHT10 humidity and temperature sensor inside the cabin. With this sensor, temperature and humidity parameters are correlated to each other. This sensor is used to detect both humidity and temperature changes in the cabin and this would be connected to an Adurino Pro processor. The processor would be preprogrammed in such a way, as to perform cut out operation and also to vary the output voltage according to the requirement.

Once mist is detected, the sensor would send a signal to the engine or electrical control unit (ECU). This in turn would complete the circuit to supply power to the electrodes and the carbon nanotube heater would start to heat the windshield. Once the sensor detects that there is no more mist on the windscreen, a feedback signal would be sent to the ECU to cut out the circuit and this would turn off the heater. By installing the above described method it is possible to create a safe driving environment. The above method can offer a superior optical transmittance and risk free driving.

7.2. Leading Edge Deicing System

Deicing on the leading edge of an aircraft can be achieved by various methods. It is very important to remove the ice from the aircraft's leading edge to prevent lift reduction. Typically, before flight, an anti-icing fluid is sprayed on the aircraft's wings but this can leave residue in critical areas such as pivot joints and mechanical linkages.

Figure 7.1 Frozen gel causes damages to the joints (Hille, 2008)

This residue can rehydrate and form a gel-like material that can cause serious restriction of movements in the primary control surfaces, as shown in Figure 7.1. This method requires serious scheduled inspection to prevent catastrophe. On-board deicing methods are available (inflatable boot, air bleed from engines etc.,) but add additional weight to the aircraft. This decreases the fuel efficiency, increases the maintenance procedures, and raises the passenger or cargo fare. Hence, adding weight is the first enemy to an economic flight. The proposed windshield defrosting method is applicable for deicing the leading edge of the aircraft wing. The principle is same for both applications. There are no moving parts because the design is simple and elegant. Unlike a windshield, optical transmittance is not a requirement, so opaque protective coatings could be used as well.

This principle does not require special manufacturing procedures or replace the existing wing. It is possible to turn the conventional aircraft leading edge into a carbon nanotube based deicing leading edge heater with minimum cost. The heaters would be applied in the form of arrays with an individual, or pattern-based, operation. These heaters are installed on a layer of nonconductive coating which is applied on the leading edge surface. This simple approach would reduce maintenance and decrease the aircraft downtime.

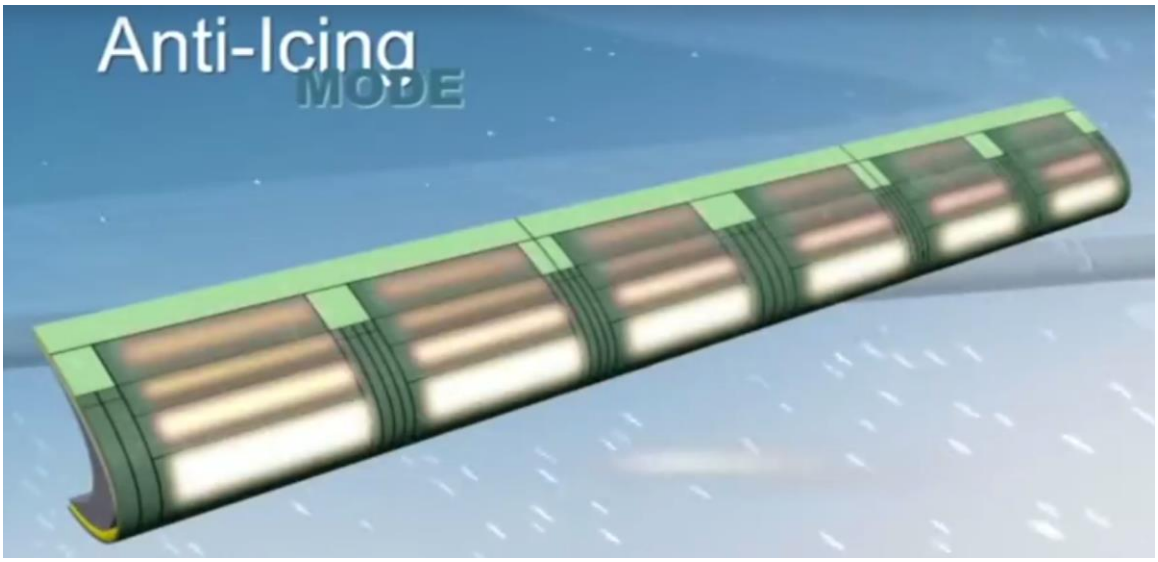

Figure 7.2 Concept of installing the deicing system in aircraft leading edges (GKN Aerospace)

7.3. Wind Turbine Blade Deicing

Wind turbines are the best reliable and renewable power source. Just like aircraft cannot fly with ice on its wing, wind turbines also cannot operate in icing conditions. In North America, about 65% of wind turbines are located in places where ice formation on the blades is possible or likely. There are no deicing techniques available for wind turbines. The only possible solution available is to shut down the wind turbine once ice is detected on the blade. The inner parts of the wind turbines are protected with specially-designed low-viscous oil, but the outer parts remain exposed to ice.

Figure 7.3 Shutdown of wind turbines due to icing problem which requires technician inspection to restart (Harper, 2011)

Once the wind turbine operation is stopped due to icing, visual inspection is necessary in order to restart. It increases the downtime, especially for wind turbines in remote locations. There are unique systems available to detect the ice and shut down the operation autonomously, but there is no system in operation to overcome the ice formation. Unfortunately, the winter months demand more energy than the rest of the year. The wind turbines have the capability to meet the power demands if they are operational at the specific time because winter is the best time to harvest wind energy. Due to icing issues, the wind turbines are not a reliable source of energy and this can be rectified by installing deicing heaters. The heaters can be applied in the form of arrays with individual or pattern-based operation. This process follows the same principle as defrosting the windshield.

8. Conclusions and Future Work

This process and experimentation fabricated a transparent glass heater with the specially engineered CNTRENE^{TM} solution. The transparent glass heater with an optical transparency of more than 90% in the visible wavelength spectrum was created using a spin coating method. A layer of CNT with a resistance of ~1.2 KΩ was obtained with proven repeatability. The manufactured specimens showed excellent performance in heating and cooling and the response was instantaneous. The specimen developed is radio frequency (RF) transparent, unlike current ITO heaters. Different protective methods were tested to create a perfect isolation environment for the carbon nanotubes. A lifetime performance test and continuous cycle test were performed and proved that there was no degradation in heating performance over time. For voltage requirements, the scalability test was performed and provided an effective way to calculate the amount of voltage.

This research can open a new possibility for heating mechanisms and develop the next-generation transparent heater. By carefully reviewing the requirement of various potential applications, this method can be applicable in different areas, such as deicing the leading edge of aircraft wing, leading edge of wind turbine blades, car windshield or aircraft windshield. This process also shows promising results for transparent flexible heaters. Future work involves testing a spray coating technique on a large scale model, and testing the full scale industrial model in an icing wind tunnel. More work also needs to be done on measuring the thickness of the applied coating, as well as the non-uniformity of the temperature profile.

REFERENCES

Ari, N., and Kribus,A., "Impact of the Peltier effect on concentrating photovoltaic cells," *Solar Energy Materials and Solar Cells*, Vol. 94, Issue 12, December 2010, Pages 2446-2450.

Barberio, M., Camarca, M., Barone, P., Bonanno, A., Oliva, A., and Xu, F., "Electric resistivity of multi-walled carbon nanotubes at high temperatures," *Surface science*, Vol. 601, No. 13, 2007, pp. 2814-2818.

Begtrup, G. E., Ray, K. G., Kessler, B. M., Yuzvinsky, T. D., Garcia, H., and Zettl, A., "Probing nanoscale solids at thermal extremes," *Physical review letters*, Vol. 99, No.15, 2007, pp. 155901-4.

Bekyarova, E., Itkis, M. E., Cabrera, N., Zhao, B., Yu, A., Gao, J., and Haddon, R. C., "Electronic properties of single-walled carbon nanotube networks," *Journal of the American Chemical Society*, Vol. 127, No. 16, 2005, pp. 5990-5995.

Briggs, M. D. U.S. Patent No. 7,928,345. Washington, DC: U.S. Patent and Trademark Office. (2011).

Carbon nanotubes: The weird world of 'remote Joule heating' (10 April 2012). Retrieved from http://phys.org/news/2012-04-carbon-nanotubes-weird-world-remote.html

Cheng, X. B., Huang, J. Q., Zhang, Q., Peng, H. J., Zhao, M. Q., and Wei, F., "Aligned carbon nanotube/sulfur composite cathodes with high sulfur content for lithium–sulfur batteries," *Nano Energy*, Vol. 4, 2014, pp. 65-72.

Coutal, C., Azema, A., and Roustan, J. C., "Fabrication and characterization of ITO thin films deposited by excimer laser evaporation," *Thin Solid Films*, Vol. 288, No. 1, 1996, pp. 248-253.

Deng, H. X., Gong, X. L., & Wang, L. H. (2006). Development of an adaptive tuned vibration absorber with magnetorheological elastomer. Smart materials and structures, 15(5), N111.

De Greef, N., Zhang, L., Magrez, A., Forró, L., Locquet, J. P., Verpoest, I., and Seo, J. W., "Direct growth of carbon nanotubes on carbon fibers: Effect of the CVD parameters on the degradation of mechanical properties of carbon fibers," *Diamond and Related Materials*, Vol. 51, 2015, pp. 39-48.

Harper, N. Detecting Ice on Wind-turbine Blades (2011, July 21). Retrieved from http://www.windpowerengineering.com/maintenance/detecting-ice-on-wind-turbine-blades/

Hille, J. Deicing and Anti-icing Fluid Residual (2008). Retrieved from http://www.boeing.com/commercial/aeromagazine/articles/qtr_1_07/article_03_1.html

Ilinca, A., "Analysis and Mitigation of Icing Effects on Wind Turbines, Wind Turbines," Dr. Ibrahim AlBahadly (Ed.), ISBN: 978-953-307-221-0, *InTech*. (2011).

Itkis, M. E., Borondics, F., Yu, A., and Haddon, R. C., "Bolometric infrared photoresponse of suspended single-walled carbon nanotube films," *Science*, Vol. 312, No. 5772, 2006, pp. 413-416.

Janas, D., and Koziol, K. K., "Improved performance of ultra-fast carbon nanotube film heaters," *Journal of Automation and Control Engineering*, Vol. 2, No. 2, 2014.

Jang, H. S., Jeon, S. K., and Nahm, S. H., "The manufacture of a transparent film heater by spinning multi-walled carbon nanotubes," *Carbon 49*, Vol. 1, 2011, pp. 111-116.

Jhi, S. H., Louie, S. G., and Cohen, M. L., "Electronic properties of oxidized carbon nanotubes," *Physical Review Letters*, Vol. 85, No. 8, 2000, pp. 1710.

Jung, D., Lee, K. H., Kim, D., Burk, D., Overzet, L. J., and Lee, G. S., "Highly conductive flexible multi-walled carbon nanotube sheet films for transparent touch screen," *Japanese Journal of Applied Physics*, Vol. 52, No.3S, 2013.

Jung, D., Kim, D., Lee, K. H., Overzet, L. J., and Lee, G. S., "Transparent film heaters using multi-walled carbon nanotube sheets," *Sensors and Actuators A: Physical*, Vol. 199, 2013, pp. 176-180.

Kang, M. G., Kim, M. S., Kim, J., and Guo, L. J., "Organic solar cells using nanoimprinted transparent metal electrodes. *Advanced Materials*, Vol. 20, No. 23, 2008, pp. 4408-4413.

Kang, T. J., Kim, T., Seo, S. M., Park, Y. J., and Kim, Y. H., "Thickness-dependent thermal resistance of a transparent glass heater with a single-walled carbon nanotube coating," *Carbon 49*, Vol. 4, 2011, pp. 1087-1093.

Kim, D., Zhu, L., Jeong, D. J., Chun, K., Bang, Y. Y., Kim, S. R., ... and Oh, S. K., "Transparent flexible heater based on hybrid of carbon nanotubes and silver nanowires," *Carbon 49*, Vol. 63, 2013, pp. 530-536.

Kumar., Mukul., and Yoshinori Ando., "Chemical vapor deposition of carbon nanotubes: a review on growth mechanism and mass production," *Journal of nanoscience and nanotechnology*, Vol. 10.6, 2010, pp. 3739-3758.

Lee, S. M., Byeon, H. J., Lee, J. H., Baek, D. H., Lee, K. H., Hong, J. S., and Lee, S. H., "Self-adhesive epidermal carbon nanotube electronics for tether-free long-term continuous recording of biosignals," *Scientific reports*, Vol. 4, 2014.

Park, T., and Kim, D., "Excimer laser sintering of indium tin oxide nanoparticles for fabricating thin films of variable thickness on flexible substrates," *Thin Solid Films*, Vol. 578, 2015, pp. 76-82.

Santini, C.A., Vereecken, P.M., Volodin, A., and De Gendt, S., "A study of Joule heating-induced breakdown of Carbon Nanotubeinterconnects," Nanotechnology 22, 2011, pp. 395202-395211.

Skouroliakou, A. S., Seferis, I., Sianoudis, I., Valais, I., Fragopoulou, A. F., and Margaritis, L. H., "Infrared Thermography Imaging: Evaluating surface emissivity and skin thermal response to IR heating," *e-Journal of Science & Technology (e-JST)*, 2014.

Soltani-kordshuli, F., Zabihi, F., and Eslamian. M., "Graphene-doped PEDOT:PSS nanocomposite thin films fabricated by conventional and substrate vibration-assisted spray coating (SVASC)," *Engineering Science and Technology, an International Journal*, 2016.

Thomas R. Tuttle, Jr., "Ammonium Hydroxide: What Is Its Structure?," *Brandeis University Waltham*. MA 02254, Vol. 8, June 1991, pp. 553.

Yang, Y., Liu, L., Tang, Y., Zhang, Y., Jia, D., and Kong, L., "Bamboo-like carbon nanotubes containing sulfur for high performance supercapacitors," *Electrochimica Acta*, Vol. 191, 2016, pp. 846-853

Yawen, C., Juanhong, W., Zhiming, Z., Zhixiong, J., and Chen, S., "Fabricating large-area white OLED lighting panels via dip-coating," *Organic Electronics*, Vol. 37, October 2016, pp. 458-464.

Yoon, Y. H., Song, J. W., Kim, D., Kim, J., Park, J. K., Oh, S. K., and Han, C. S., "Transparent Film Heater Using Single-Walled Carbon Nanotubes," *Advanced Materials*, Vol. 19, No. 23, 2007, pp. 4284-4287.

Yu, X., Rajamani, R., Stelson, K. A., and Cui, T., "Carbon nanotube-based transparent thin film acoustic actuators and sensors," *Sensors and Actuators A: Physical*, Vol. 132,No. 2, 2006, pp. 626-631.

Wang, Y. Q., and Liu, L., Beijing Funate Innovation Technology Co., Ltd., Washington, DC, U.S. Patent Application for a "Carbon nanotube defrost windows," No. 8426776, filled on 29 Dec. 2009.

World's first electro-thermal ice protection system for a civil aircraft – for the B-787 - successfully completes icing tunnel tests. Retrieved from http://www.gkn.com/aerospace/media/news/Pages/World%E2%80%99s-first-electro-thermal-ice-protection-system-for-a-civil-aircraft.aspx#sthash.lTkqJrDE.dpuf

Wu, Z., Chen, Z., Du, X., Logan, J. M., Sippel, J., Nikolou, M., ... and Rinzler, A. G., "Transparent, conductive carbon nanotube films," *Science*, Vol. 305, No. 5688, 2004, pp. 1273-1276

A. Observation of Experiments

Exp-Number	RPM1/ RPM2	Time (seconds)	Number layers	Dimension	Comments	Transmi-ttance (%)	Resistance k ohm
11	0/2000	30	1	25 × 25 mm	Evenly coated	98	100
12	0/2000	30	2	25 × 25 mm	The coating is not to perfect. Visible non-uniformity	96	70
13	0/2000	30	3	25 × 25 mm	Coating looks perfect. Transmittance is less when compared to the slide 12	95	10
14	0/2000	30	4	25 × 25 mm	Coating looks perfect. Transmittance is less when compared to the slide 13	94	7
15	0/2000	30	5	25 × 25 mm	Transmittance is less when compared to the slide 14	93	5
16	0/2000	30	2	25 × 25 mm	-	97	70
17	0/2000	30	3	25 × 25 mm	-	96	13
18	0/2000	30	4	25 × 25 mm	-	94	8
19	0/2000	30	5	25 × 25 mm	-	93	5
20	0/2000	30	2	25 × 25 mm	-	97	25
21	0/2000	30	3	25 × 25 mm	-	95	13
22	0/2000	30	4	25 × 25 mm	-	94	81
23	0/2000	30	5	25 × 25 mm	-	92	7
24	0/2000	30	5	25 × 25 mm	-	93	3

25	0/2000	30	5	25 × 25 mm	-	92	N/A
26	0/2000	30	6	25 × 25 mm	The layer is not perfect. Some blotches are observed	92	3
27	0/2000	30	7	25 × 25 mm	The layer is not perfect. Some blotches are observed	91	2
28	0/2000	30	8	25 × 25 mm	The layer is not perfect. Some blotches are observed.	88	1.5
29	0/2000	30	9	25 × 25 mm	The layer is uniform. No blotches are observed.	87	1.3
30	0/2000	30	10	25 × 25 mm	The layer is not perfect. Some blotches are observed.	86	1.2
Gold plated				25 × 25 mm	Sputter coated	0.2	
31	0/2000	30	5	25 × 50 mm	The coating is not uniform	93.4	3.2
32	0/2000	30	5	25 × 50 mm	Rectangular slide 25 by 50 mm	93.4	4.1
33	0/2000	30	5	25 × 50 mm	Coating is pretty good	93.7	3.2
34	0/2000	30	5	25 × 50 mm		94.1	3.4
35	0/2000	30	5	25 × 75 mm	No defects	93.8	5.2
36	0/2000	30	5	25 × 75 mm	No defects	93.6	5.3
37	0/2000	30	5	25 × 75 mm	No defects	93.6	5.1

Annealed glass	0/1500	30	4	2” × 2”	The coating is uniform and the repeatability is good.	94.2	7.3
Tempered glass	0/1500	30	4	2” × 2”	Looks good	94.1	7.9
Laminated glass	0/1500	30	4	2” × 2”	The transmittance of this glass is unpredictable	96.7	7.1
CNTRENE™ expired on 7/14/2016. Tested for further shelf-life.							
41	0/2000	30	5	25 × 75 mm	The coating is perfect	92	5.1
42	0/2000	30	5	25 × 75 mm	There are some blotches	93	5.4
43	0/2000	30	5	25 × 75 mm	Looks good	93	4.9
44	0/2000	30	5	25 × 75 mm	Coating is uniform	92	5.2
45	0/2000	30	5	25 × 75 mm	Looks good	93	5.1

B. MATLAB Code

Number of Layers Vs Resistance

```
xaxis = test5(:,1);
yaxis = test5(:,2);
plot(xaxis,yaxis,'-ok','linewidth', 2)
title('Number of layers VS resistance')
xlabel('Number of layers (N)')
ylabel('Resistance (K \Omega)')
```

Temperature Vs Resistance

```
xaxis = test3(:,1);
yaxis = test3(:,2);
plot(xaxis,yaxis,'-ok','linewidth', 2)
title('Number of layers VS resistance')
xlabel('Temperature ^{\circ}C','Interpreter','tex')
ylabel('Resistance (K \Omega)')
```

Number of Layers Vs Transmittance

```
xaxis = test2(:,1);
yaxis = test2(:,2);
plot(xaxis,yaxis,'-ok','linewidth', 2)
title('Number of layers VS Transmittance')
xlabel('Number of layers (N)')
ylabel('Transmittance %')
axis([0 10 86 100])
```

Time Profile Vs Temperature

```
x = test5(:,2);
y = test5(:,1);
plot(x,y,'r','linewidth', 3)
title('Continuous Cycle Test')
xlabel('Relative Time (seconds)')
ylabel('Temperature ^{\circ}C','Interpreter','tex')
axis([0 2200 28 61])
```

Week Vs Temperature

```
x = test4(:,1);
y = test4(:,2);
x1 = test5(:,1);
y1 = test5(:,2);
x2 = test6(:,1);
y2 = test6(:,2);
Figure
subplot(3,1,1)
plot(x,y,'k*-','linewidth', 2)
axis([0 10 40 100])
xlabel('week')
title('# 15 5 CNT layer Slide Temperature Trend')
ylabel('Temperature ^{\circ}C','Interpreter','tex')

subplot(3,1,2)
plot(x1,y1,'k*-','linewidth', 2)
axis([0 10 40 100])
title('# 23 5 CNT layer Slide Temperature Trend')
xlabel('week')
ylabel('Temperature ^{\circ}C','Interpreter','tex')

subplot(3,1,3)
plot(x2,y2,'k*-','linewidth', 2)
title('# 29 5 CNT layer Slide Temperature Trend')
xlabel('week')
ylabel('Temperature ^{\circ}C','Interpreter','tex')
axis([0 8 80 140])
```

Thickness Vs Time

```
xaxis = test1(:,1);
yaxis = test1(:,2);
x1axis = test2(:,1);
y1axis = test2(:,2);
x2axis = test3(:,1);
y2axis = test3(:,2);
plot(xaxis,yaxis,x2axis,y2axis,x1axis,y1axis,'LineWidth', 2)
title('Number of layers VS resistance')
xlabel('Time (seconds)')
ylabel('Temperature ^{\circ}C','Interpreter','tex')
axis([0 250 25 110])
title('Temperature vs Time profile for 4, 6 and 7 layers')
legend('4 layer','6 layer','7 layer','Location','southeast')
xt = [150 150 150];
yt = [89 106.5 75];
str = {'~4.97µm','~8.19µm','~2.51µm'};
text(xt,yt,str)
```

Multi-plot

```
xaxis = test(:,1);
yaxis = test(:,2);
x1axis = test(:,4);
y1axis = test(:,5);
x2axis = test(:,7);
y2axis = test(:,8);
x3axis = test(:,10);
y3axis = test(:,11);
x4axis = test(:,13);
y4axis = test(:,14);
x5axis = test(:,16);
y5axis = test(:,17);
x6axis = test(:,19);
y6axis = test(:,20);
x7axis = test(:,22);
y7axis = test(:,23);
x8axis = test(:,25);
y8axis = test(:,26);

plot(xaxis,yaxis,x1axis,y1axis,x2axis,y2axis,x3axis,y3axis,x4axis,y4ax
is,x5axis,y5axis,x6axis,y6axis,x7axis,y7axis,'g',x8axis,y8axis,'--
k','LineWidth', 2)
title('Number of layers VS resistance')
xlabel('Time (seconds)')
ylabel('Temperature ^{\circ}C','Interpreter','tex')
axis([0 250 25 70])
title('Temperature vs Time profile for 4, 6 and 7 layers')
legend('Point1','Point2','Point3','Point4','Point5','Point6','Point7',
'Point8','Point9','Location','southeast')
% xt = [150 150 150 150 150 150 160 150 220];
% yt = [51 47 45.5 65 57 49 52.5 50 48.5];
% str =
{'Point1','Point2','Point3','Point4','Point5','Point6','Point7','Point
8','Point9'};
% text(xt,yt,str)
```

Heat spot Image Processing

```
close all;
img_src=imread('2.png');
ref=imread('1.png');

imgr=img_src(:,:,1);
imgg=img_src(:,:,2);
imgb=img_src(:,:,3);

imgr2=ref(:,:,1);
imgg2=ref(:,:,2);
imgb2=ref(:,:,3);

Hnimgr= imhist(imgr);
Hnimgg= imhist(imgg);
Hnimgb= imhist(imgb);

Hnimgr2= imhist(imgr2);
Hnimgg2= imhist(imgg2);
Hnimgb2= imhist(imgb2);

outr=histeq(imgr,Hnimgr2);
outg=histeq(imgg,Hnimgg2);
outb=histeq(imgb,Hnimgb2);

histsp(:,:,1)=outr;
histsp(:,:,2)=outg;
histsp(:,:,3)=outb;

Figure;
subplot(221);imshow(ref);title('before');
subplot(222);imshow(img_src);title('after');
subplot(224);imshow(histsp);title('result');

%plot for histogram
Figure;
subplot(322);plot(Hnimgr);title('Red after');
xlabel('Light Intensity');
ylabel('Number of Pixels');
subplot(324);plot(Hnimgg);title('Green after');
xlabel('Light Intensity');
ylabel('Number of Pixels');
subplot(326);plot(Hnimgb);title('Blue after');
xlabel('Light Intensity');
ylabel('Number of Pixels');
subplot(321);plot(Hnimgr2);title('Red before');
```

```
xlabel('Light Intensity');
ylabel('Number of Pixels');
subplot(323);plot(Hnimgg2);title('Green before');
xlabel('Light Intensity');
ylabel('Number of Pixels');
subplot(325);plot(Hnimgb2);title('Blue before');
xlabel('Light Intensity');
ylabel('Number of Pixels');
Figure;
subplot(131);imhist(outr);title('Red Result');
xlabel('Light Intensity');
ylabel('Number of Pixels');
subplot(132);imhist(outg);title('Green Result');
xlabel('Light Intensity');
ylabel('Number of Pixels');
subplot(133);imhist(outb);title('Blue Result');
xlabel('Light Intensity');
ylabel('Number of Pixels');
```